Constitutive modelling of state-dependent behaviour of unsaturated soils: an overview

Authors: C. W. W. Ng, C. Zhou* and C.F. Chiu

*Corresponding author

Author's affiliation and address:

Name: Charles Wang Wai Ng

Title: CLP Holdings Professor of Sustainability

Affiliation: Department of Civil and Environmental Engineering, Hong Kong University of Science and Technology, Clear Water Bay, Hong Kong

E-mail: cecwwng@ust.hk

Name: Chao Zhou

Title: Assistant Professor

Affiliation: Department of Civil and Environmental Engineering, The Hong Kong Polytechnic University, Hung Hom, Hong Kong

E-mail: c.zhou@polyu.edu.hk

Name: Abraham Chung Fai Chiu

Title: Professor

Affiliation: Department of Civil and Environmental Engineering, Shantou University, China

E-mail: acf_chiu@stu.edu.cn

Abstract

An unsaturated soil is a three-phase material that is ubiquitous on the earth's surface. The fully saturated and completely dry states are just two limiting conditions of an unsaturated soil. The state and properties of unsaturated soils can change significantly with external loads, weather conditions and groundwater level. Proper modelling of the state-dependent behaviour of unsaturated soils is crucial for analysing the performance of almost all civil engineering structures. So far, there are many unsaturated soil models and several relevant review papers in the literature. None of the existing review papers, however, focused on the state-dependency of unsaturated soil behaviour. Moreover, some aspects of soil behaviour have not been reviewed, including small strain stiffness, dilatancy and stress-dependence of water retention curve. In the current review paper, the state-dependency of unsaturated soil behaviour is reviewed, with a particular attention to the three missing parts. The review is carried out in a unified and relatively simple constitutive framework, which adopts a three-by-three compliance matrix to link incremental volumetric strain, deviator strain and degree of saturation to incremental mean net stress, deviator stress and suction. All of the nine variables in the proposed three-by-three compliance matrix have clear physical meanings and can be measured through compression, shearing and water retention tests. Theoretical models based on other constitutive stress variables can be also converted to this framework by matrix transformation.

Keywords: unsaturated soil; constitutive modelling; state-dependency; hydromechanical coupling

1 Introduction

Soil is a porous medium in which the pores between solid grains play an important role in governing its mechanical and hydraulic behaviour. The pores can be filled up with liquid and/or gas. Many classical theories of soil mechanics have been developed based on the assumptions that the pores are filled up with either liquid (i.e. fully saturated) or gas (i.e. completely dry), e.g. Terzaghi's theory of one dimensional consolidation, Rankine's theory of earth pressure, among others. However, fully saturated and completely dry states are only two limiting conditions of soils [57]. In many geotechnical engineering applications, the degree of saturation lies between zero and one. Many phenomena observed in unsaturated soils cannot be explained adequately by the classical theories of soil mechanics, leading to the emergence of unsaturated soil mechanics over the past few decades (e.g., [1, 11, 22, 29, 46, 57, 66, 68, 79, 84, 92, 97, 100, 104, 107]).

Since the pioneering work in the 1950s and 1960s to develop different laboratory techniques to control suction and to test unsaturated soils [8, 17, 35, 55, 67], the contributions of suction to the mechanical and hydraulic behaviour of unsaturated soils have been better understood. The theoretical development of constitutive models for unsaturated soils lags behind the corresponding laboratory studies. So far, several reviews on the constitutive models for unsaturated soils are available in the literature [19, 32, 80, 82, 91]. These reviews discussed some of the important aspects of constitutive modelling of unsaturated soils, such as constitutive variables, wetting-induced collapse, compressibility, yielding, shear strength, failure criteria, water retention behaviour and hydromechanical coupling. The different aspects of unsaturated soil behaviour were not reviewed and discussed in a unified theoretical framework. Moreover, some issues were relatively less discussed, including state-dependent small strain stiffness, dilation and stress-dependent water retention behaviour.

In this study, a unified and relatively simple constitutive framework is presented for unsaturated soils. This framework adopts a three-by-three compliance matrix to link volumetric strain, deviator strain and incremental degree of saturation to incremental mean net stress, deviator stress and suction. All of the nine variables in the compliance matrix have clear physical meanings, which are illustrated throughout by various unsaturated soil tests. Based on this constitutive framework, the modelling of state-dependent behaviour of unsaturated soils is reviewed in a systematic approach.

2 A unified and simple framework for the state-dependent behaviour of unsaturated soils

In the constitutive modelling of unsaturated soils, one of the key issues is the choice of proper constitutive variables. Many different constitutive stress variables have been proposed in the literature to model the mechanical behaviour of unsaturated soils (e.g. [21, 77, 92]). Gens et al. [32] reviewed the different variables adopted in existing elastoplastic models. They believed that "*Different constitutive stresses stand on an equal footing and the matter of adopting one or the other must be decided using the criteria of convenience*." In the unified and simple framework of this current review, net stress and matric suction are used for simplicity. Net stress is defined as the difference between total stress (σ) and pore air pressure (u_a). Matric suction is calculated as the difference between pore air and pore water pressure (u_w), and it is referred to as suction for simplicity in the following paragraphs.

By adopting net stress and suction, the constitutive formulations for an unsaturated soil can be expressed in a general incremental form as follows:

$$\begin{bmatrix} \mathrm{d}\varepsilon_{\mathrm{v}} \\ \mathrm{d}\varepsilon_{\mathrm{q}} \\ \mathrm{d}S_{\mathrm{r}} \end{bmatrix} = \begin{bmatrix} I_{11} & I_{12} & I_{13} \\ I_{21} & I_{22} & I_{23} \\ I_{31} & I_{32} & I_{33} \end{bmatrix} \begin{bmatrix} \mathrm{d}p \\ \mathrm{d}q \\ \mathrm{d}s \end{bmatrix} \tag{1}$$

where dε_v is the increment in volumetric strain; dε_q is the increment in deviator strain; dS_r is the increment in the degree of saturation; dp is the increment in the mean net stress; dq is the increment in the deviator stress; ds is the increment in suction; and I_{ij} (i = 1, 2 and 3; j = 1, 2 and 3) are state-dependent variables for a given soil. According to equation (1), the variables I_{11}, I_{21}, and I_{31} in the compliance matrix describe the behaviour of unsaturated soils during compression, including the development of volumetric strain, deviator strain and degree of saturation. Similarly, I_{12}, I_{22}, and I_{32} describe the hydromechanical behaviour during the shearing process, while I_{13}, I_{23} and I_{33} capture the behaviour of soil subjected to drying/wetting. All nine variables can be calibrated through suction- and stress-controlled tests on unsaturated soils. These variables can be also determined by using constitutive formulations for the compression, shearing and water retention behaviour of unsaturated soils, as discussed later. Equation (1) is still valid when soil is saturated, which is considered as a special case of unsaturated soil with S_r = 100%. At this special condition, the net stress should be replaced by the Terzaghi's effective stress and the values of I_{13}, I_{23}, I_{31}, I_{32} and I_{33} become zero.

Some unsaturated soil models in the literature are based on other constitutive stress variables rather than net stress and suction. These models can be also converted to equation (1) by matrix transformation. In any constitutive model, the relationship between strain increment $\{\mathbf{d\hat{\varepsilon}}\}$ and stress increment $\{\mathbf{d\hat{\sigma}}^*\}$ can be described using a general formulation:

$$\{\mathrm{d}\hat{\boldsymbol{\varepsilon}}\} = [\boldsymbol{C}*]\{\mathrm{d}\hat{\boldsymbol{\sigma}}*\} \tag{2}$$

where $[\mathbf{C}^*]$ is the compliance matrix; $\{\hat{\boldsymbol{\sigma}}^*\}$ and $\{\hat{\boldsymbol{\varepsilon}}\}$ are the constitutive stress and strain variables, respectively. For the discussion here, the strain variables $\{\hat{\boldsymbol{\varepsilon}}\}$ is defined as $\{\varepsilon_v, \varepsilon_q, S_r\}$ in all models. To obtain the relationship between $[\mathbf{C}^*]$ and $[\mathbf{C}]$ (i.e., the compliance matrix defined in equation (1)), $\{\mathrm{d}\hat{\boldsymbol{\sigma}}^*\}$ can be expressed as [10]

$$\{\mathrm{d}\hat{\boldsymbol{\sigma}}^*\} = [\boldsymbol{T}_\mathbf{a}]\{\mathrm{d}\hat{\boldsymbol{\sigma}}\} + [\boldsymbol{T}_\mathbf{b}]\{\mathrm{d}\hat{\boldsymbol{\varepsilon}}\} \tag{3}$$

where $\{\mathrm{d}\hat{\boldsymbol{\sigma}}\}$ is the incremental form of constitutive stress variables $\{\mathrm{dp}, \mathrm{d}q, \mathrm{d}s\}$ used in equation (1); $[\mathbf{T}_{\boldsymbol{a}}]$ and $[\mathbf{T}_\mathbf{b}]$ are two matrixes and their values depend on the constitutive stress variables in the constitutive model investigated. Substituting equations (1) and (3) into equation (2), it is obtained that

$$[\boldsymbol{C}] = [\boldsymbol{I} - \boldsymbol{C}^*\boldsymbol{T}_\mathbf{b}]^{-1}[\boldsymbol{C}^*][\boldsymbol{T}_\mathbf{a}] \tag{4}$$

where $[\mathbf{I}]$ is a unit matrix. It should be noted that equations (2) and (4) are general equations. They can be used to convert any constitutive model to equation (1). When different models are used, however, $[\mathbf{T}_\mathbf{a}]$ and $[\mathbf{T}_\mathbf{b}]$ take different forms. For example, the model of Wheeler et al. [92] uses the following three constitutive stress variables: $\{\hat{\boldsymbol{\sigma}}^*\} = \{p^*, q, s^*\}$, where the Bishop's stress p^* and modified suction s^* are defined as $(p + sS_\mathrm{r})$ and (ns), respectively. From the incremental form of $\{\hat{\boldsymbol{\sigma}}^*\}$, it can be readily derived that:

$$[\boldsymbol{T}_\mathbf{a}] = \begin{bmatrix} 1 & 0 & S_\mathrm{r} \\ 0 & 1 & 0 \\ 0 & 0 & n \end{bmatrix} \tag{5}$$

$$[\boldsymbol{T}_\mathbf{b}] = \begin{bmatrix} 0 & 0 & s \\ 0 & 0 & 0 \\ (1-n)s & 0 & 0 \end{bmatrix} \tag{6}$$

Another example is the model of Khalili et al. [39], which adopts the following constitutive stress variables: $\{\hat{\boldsymbol{\sigma}}^*\} = \{p_\mathrm{k}^*, q, s\}$. p_k^* is the mean effective stress proposed by Khalili and Khabbaz [40]: $(p + \chi s)$, where χ is defined as follow:

$$\chi = \begin{cases} 1 & for\ s \le s_\mathrm{e} \\ \left(\frac{s}{s_\mathrm{e}}\right)^{-0.55} & for\ s > s_\mathrm{e} \end{cases} \tag{7}$$

where s_e is the suction value marking the transition between saturated and unsaturated states. $[\mathbf{T}_\mathbf{a}]$ and $[\mathbf{T}_\mathbf{b}]$ are calculated using the following two equations:

$$[\boldsymbol{T}_\mathbf{a}] = \begin{bmatrix} 1 & 0 & 2(s/s_\mathrm{e})^{-0.55} \\ 0 & 1 & 0 \\ 0 & 0 & 1 \end{bmatrix} \tag{8}$$

$$[\boldsymbol{T}_\mathbf{b}] = \begin{bmatrix} 0 & 0 & (s/s_\mathrm{e})^{0.45}(\partial s_\mathrm{e}/\partial \varepsilon_\mathrm{v}) \\ 0 & 0 & 0 \\ 0 & 0 & 0 \end{bmatrix} \tag{9}$$

Lu et al. [47] proposed a new effective stress formulation $(\sigma - \sigma^\mathrm{s})$ based on the concept of suction stress σ^s [48]. For constitutive models based on this effective stress formulation, $[\mathbf{T}_\mathbf{a}]$ and $[\mathbf{T}_\mathbf{b}]$ are calculated using the following two equations:

$$[\boldsymbol{T}_{\mathbf{a}}] = \begin{bmatrix} 1 & 0 & (S_{\mathrm{r}} - S_{\mathrm{rr}})/(1 - S_{\mathrm{rr}}) \\ 0 & 1 & 0 \\ 0 & 0 & 1 \end{bmatrix} \tag{10}$$

$$[\boldsymbol{T}_{\mathbf{b}}] = \begin{bmatrix} 0 & 0 & (S_{\mathrm{r}} - S_{\mathrm{rr}})/(1 - S_{\mathrm{rr}}) \\ 0 & 0 & 0 \\ 0 & 0 & 0 \end{bmatrix} \tag{11}$$

where S_{rr} is the residual degree of saturation. The above three examples clearly show that all constitutive models can be converted to equation (1) by matrix transformation. Within this unified framework (i.e., equation (1)), the constitutive formulations for unsaturated soil behaviour are reviewed in the following paragraphs.

2.1 Determination of the variable I_{11}

The variable I_{11} in equation (1) can be determined using the following equation:

$$I_{11} = \frac{\partial \varepsilon_{\mathrm{v}}}{\partial p} \tag{12}$$

According to equation (12), the variable I_{11} is the ratio of incremental volumetric strain to incremental mean net stress when q and s are constant. The value of this variable corresponds to soil volumetric compressibility, which can be measured through compression tests at constant q and s condition. For example, Ng and Yung [64] carried out a series of suction-controlled isotropic compression tests on a compacted completely decomposed tuff (CDT, a silt). Four suction levels, 0, 50, 100 and 200 kPa, were considered and applied. Fig. 1 shows the measured relationship between volumetric strain and mean net stress. One of the key findings was that the measured compressibility decreased with increasing suction in the stress and suction ranges considered, due to the stiffening effects of water meniscus. This observation implies that the value of I_{11} is lower at a higher suction. In contrast, some other soils have been found to be more compressible at a higher suction (e.g., Wheeler and Sivakumar [93]), probably because drying a soil would result in more compressible macro pores [26, 104]. These differing trends suggest that to obtain the value of I_{11} accurately, suction-controlled compression tests should be carried out.

To model the volume change behaviour of unsaturated soils during loading and unloading process, various formulations have been reported in the literature. They were compared and discussed by Sheng [80] in detail. To illustrate the relationship between volume change behaviour and equation (1), this current study adopts the following equation as an example:

$$de = \frac{\alpha_{\mathrm{p}}(\mathrm{s})\mathrm{d}p}{p} \tag{13}$$

Where e is the void ratio; $\alpha_{\mathrm{p}}(\mathrm{s})$ is the compressibility. It should be noted that although equation (1) does not explicitly consider yield surface, the values of variables such as I_{11} are affected by it. For unloading/reloading inside the yield surface and loading on the yield surface, $\alpha_p(s)$ are equal to $\kappa(s)$ and $\lambda(s)$ respectively. Equation (13) assumes that the compression behaviour of an unsaturated soil can be described by a straight line in the e-ln p plane. This equation has been widely used in elastoplastic models (e.g., Chiu and Ng [15]), mainly because it is simple but effective in modelling the volume change behaviour of unsaturated soils.

Based on equations (12) and (13), the following equation can be derived:

$$I_{11} = \frac{\alpha_p(s)}{(1+e)p} \tag{14}$$

Equation (14) clearly reveals that the value of I_{11} is affected by net stress, suction and the void ratio. Therefore, the state-dependent compressibility is considered by this equation and hence by equation (1).

2.2 Determination of the variable I_{12}

According to equation (1), the variable I_{12} is described by

$$I_{12} = \frac{\partial \varepsilon_v}{\partial q} \tag{15}$$

It is the ratio of incremental volumetric strain to incremental deviator stress when p and s are constant. Volumetric strain can be induced by dilation/contraction during the shearing process, which is irreversible (i.e., the elastic volumetric strain is equal to zero). Hence,

$$\mathrm{d}\varepsilon_v = \left(\mathrm{d}\varepsilon_q - \frac{\mathrm{d}q}{G_0}\right) D_q \tag{16}$$

where G_0 is the elastic shear modulus; and D_q is the dilatancy associated with the plastic mechanism of shearing. From equations (15) and (16), the following equation can be derived:

$$I_{12} = \left(\frac{\partial \varepsilon_q}{\partial q} - \frac{1}{G_0}\right) D_q \tag{17}$$

where $\partial\varepsilon_q/\partial q$ is defined as I_{22}. Equation (17) suggests that the value of I_{12} is governed by three variables, I_{22}, G_0 and D_q. The variable D_q is discussed here, whereas detailed discussion on I_{22} and G_0 are given later.

Ng and Chiu [53, 54] carried out two series of triaxial tests on compacted decomposed volcanic (CDV, a silty clay) and compacted decomposed granitic (CDG, a sand silt) soils. Triaxial undrained and constant water content tests were conducted on saturated and unsaturated specimens, respectively. They found that a higher stress ratio is required to mobilise the same amount of dilatancy when the suction is higher. A similar behaviour was found for the CDG soil. Ng and Zhou [69] reported a series of suction-controlled direct shear tests on another coarse-grained CDG soil. For the five tested specimens, specimens subjected to suctions of 200 and 400 kPa exhibited brittle stress–strain behaviour, while the other three specimens at suctions of 0, 10 and 50 kPa exhibited ductile behaviour.

All four unsaturated specimens exhibited a phase transformation from positive to negative dilatancy with increasing stress ratio. It was also observed that the stress ratio corresponding to a maximum negative dilatancy increased with suction. Besides, the maximum negative dilatancy decreased (i.e., the soil became more dilative) with increasing suction. Through microscopic analysis, Ng et al. [61] have illustrated that suction-induced dilatancy is not governed by a change in void ratio, but depends on suction effects on the micro and macro pores. Based on the above experimental results, it is evident that the dilatancy of unsaturated soils depends on suction. As a consequence, the formulations developed for saturated soils should be modified for unsaturated soils.

Dilatancy equation (or plastic flow rule) is one of the essential components of a constitutive model for unsaturated soils. Alonso et al. [1] has presented one of the first elastoplastic models for unsaturated soils. This model is commonly referred to as the Barcelona basic model (BBM), which adopts the Modified Cam Clay model (MCCM) as the reference model at the saturated state. Hence, the yield curve is an ellipse at constant suction associated to a preconsolidation stress p_0 (or yield stress), which increases with increasing suction. The relationship between p_0 and suction is referred to as the loading–collapse (LC) curve in the BBM. It should be noted that the shape of LC curve depends on the isotropic compression lines at different values of suction. In the three–dimensional stress and suction space, the yield surface is a series of ellipse. As the associated flow rule is used in the MCCM, the plastic potential function is the same as the yield curve. However, the MCCM over–predicts the volumetric deformation at K_0 condition [31]. Thus, a non-associated flow rule is adopted in the BBM (see equation (A1) in Table 1). A parameter α is used such that no lateral strain is predicted from equation (A1) under K_0 condition. p_s is a parameter describing the contribution of suction on the tensile strength of unsaturated soil. In equation (A1) parameters p_0 and p_s are functions of suction. Thus, the contribution of suction on the dilatancy is taken into account by these two parameters. If the stress states of a soil lie on a yield curve corresponding to a suction s_1 for a given stress ratio η, the same stress states of soil will lie inside a yield curve corresponding to a higher suction s_2 ($s_2 > s_1$). In other words, the soil subjected to suction s_2 is modelled as an overconsolidated soil in the BMM. The elasticity and equation (A1) are used to predict the shear–induced volume change when the stress states lie inside and on the current yield surface, respectively. Besides, a higher stress is required to reach the zero dilatancy at the critical state for soil subjected to a higher suction (i.e. a higher p_s).

Due to the inherent shortcomings of the MCCM, the BBM and the other models derived from the MCCM also cannot predict satisfactorily the shear-induced volumetric behaviour of unsaturated granular and overconsolidated soils. Two different approaches can be identified to address this limitation. In the first approach, different dilatancy equations for saturated sand have been modified for unsaturated soils [2, 9, 15, 18]. In the second approach, new constitutive models have been developed based on the bounding surface plasticity [52]and sub-loading surface plasticity [49, 101] to model the dilatancy of unsaturated overconsolidated soil. Cui and Delage [18] used the Nova–Wood equation (see equation (A2) in Table 1), where η_r is the stress ratio at zero dilatancy. It should be noted that η_r corresponds to not only the stress ratio at the critical state, but also the stress ratio at the phase transformation state, i.e., it changes from contractive to dilative behavior for an overconsolidated soil. η_r is dependent on both suction and stress. Two of the key limitations of their equation are that: (1) a finite dilatancy ($d = \eta_r / \mu$) is predicted for isotropic compression ($\eta = 0$); and (2) the effects of density on dilatancy are not considered.

To improve the modelling of unsaturated soil dilatancy, Chiu and Ng [15] extended the framework of state-dependent dilatancy [45] from saturated to unsaturated conditions. In their formulation (i.e., denoted as equation (A3) in Table 1), $d_1(s)$ is a model parameter that is a function of suction, and ψ is the state parameter defined as the difference between the current void ratio and the void ratio at the critical state for a given mean stress [6]. The state parameter describes the density and stress level of soils. Based on the experimental evidences [53, 54], Chiu and Ng [15] revealed that ψ is a function of density, mean net stress and suction for unsaturated soils. They illustrated that by using a single set of model parameters, equation (A3) can capture the shearing-induced volume changes of unsaturated CDV and CDG soils with different initial densities and confining pressures well. Russell and Khalili [77] alsoused ψ in the formulation of dilatancy for a boundary surface plasticity model as depicted in equation (A4). The model parameters k_d may vary for different soils, which would be assumed as a material constant if high precision simulations are not required. When k_d becomes zero, the dilatancy equation of Cam Clay is recovered. Chávez and Alonso [9] have also adopted a similar state–dependent dilatancy framework [90] in their constitutive model. The dilatancy angle φ_m is expressed as equation (A5) in Table 1, where ϕ_m = mobilised friction angle; ϕ_{cr} = friction angle at the critical state; e and e_{cr} = current void ratio and void ratio at the critical state for a given mean stress and β = model parameter. In the equation, ϕ_{cr} and e_{cr} both depend on suction. A major assumption of the three models proposed in Chiu and Ng [15], Russell and Khalili [77] and Chávez and Alonso [9] is that the tested materials can reach the critical state after large shear deformation for the range of suction studied. The triaxial test results of compacted DV and DG soils can support such hypothesis (Ng and Chiu [53, 54]). On the other hand, the experimental results of compacted shale and limestone gravels did not reach the critical state after shearing to large deformation [2, 9]. Thus, Alonso et al. [2] has proposed an alternative parameter, the plastic work input (W^p) to describe the dilatancy. It is found that equation (A6) in Table 1 gives a good fit to the measured dilatancy for the suction–controlled triaxial tests conducted on the compacted limestone gravel. In the equation, $\eta W^p/p$ is a dimensionless parameter. The effect of confining pressure p on the constraint of dilatancy is considered in the parameter. Besides, η is added such that equation (A6) can predict an infinite value of dilatancy at the isotropic compression, i.e. $\eta = 0$. Parameters a and b are two fitting variables that are functions of total suction. In the second approach, some recent constitutive models still adopted the yield function and plastic potential of MCCM, but were developed based on the bounding surface plasticity [52] and sub-loading surface plasticity [101] to model the dilatancy of unsaturated overconsolidated soil. Morvan et al. [52] extended Bardet's boundary surface model [5] for saturated soil to unsaturated soil. In this series of constitutive models, a limit state line (LSL) is defined which represents an upper bound for the admissible stress domain. The hardening modulus is formulated as a function of the stress ratio of LSL, which influences the amplitude of dilatancy and post-peak softening. Zhou and Sheng [101] adopted the framework of sub-loading surface plasticity to model the effect of initial density on the mechanical behaviour of unsaturated soil. In this model, an unified hardening (UH) parameter proposed by Yao et al. [98] was used to model the hardening of the yield surface. UH parameter depends on the similarity ratio (R) between the sub-loading surface and the reference yield surface. If the soil is normally consolidated and overconsolidated, R will be equal to 1 and less than 1, respectively. The magnitude of dilatancy and post-peak softening depend on R. Recently, Luo et al. [49] proposed a new function for the UH parameter including a state variable that describes the degree of overconsolidation under the current void ratio with reference to the anisotropic consolidation line. This state variable increases with increasing degree of overconsolidation, which controls the amount of strain softening and shear induced dilatancy.

Fig. 2 shows the measured and calculated values of dilatancy during shearing. The measurements were obtained from two triaxial tests on a gravelly sand at suctions of 0 and 40 kPa [53]. Two specimens were consolidated to the same confining pressure and similar void ratio but different suction before shearing. Theoretical results were calculated using equations (A1) to (A4) in Table 1. The value of model parameters is summarized in Table 2. It is clear that equation (A1) [1] overestimates the dilatancy of the gravelly sand, as expected. This is mainly because the model of Alonso et al. [1] was developed based on the modified Cam Clay model, which was originally proposed based on the test results of reconstituted clay. The theoretical results calculated using equations (A2) to (A4) are generally consistent with the trend of experimental data. All of these three equations were modified from the Rowe's dilatancy equation. Equation (A2) cannot take into account of density effects. Thus, a new set of parameters have to be calibrated for different densities. Khalili et al. [39] also adopted equation (A2) in a coupled flow deformation model, but formulated in an effective stress using the χ parameter as presented in equation (7). The merit of using effective stress approach is the parameters are independent of suction. On the contrary, both equations A3 [15] and A4 [9] consider the effects of density. For modelling the effect of state, (A3) and (A4) adopt the variables (e-e_c) and (e/e_c) respectively, where e and e_c are the current void ratio and void ratio at critical state respectively. It seems that equation (A3) gives better prediction of the experimental results, particularly in the range of stress ratio below 0.6. On the other hand, all these equations do not explicitly consider the influence of suction path. Some researchers found that at the same suction, the values of shearing-induced dilatancy are obliviously different along the drying and wetting paths [10, 12, 33]. Effects of suction path on soil dilatancy need more experimental and theoretical studies in the future.

One of the existing formulations for dilatancy can be used to determine I_{12}. Taking equation (A3) as an example here, based on equations (15) through (17), the following equation can be derived:

$$I_{12} = (I_{22} - 1/G_0)d_1(\mathrm{s})\left(\exp\left(m\psi\right) - \frac{\eta}{M}\right) \tag{18}$$

According to equation (18), the value of I_{12} is affected by suction. Therefore, the state-dependent dilatancy of unsaturated soils is considered by this equation and hence by equation (1).

2.3 Determination of the variable I_{13}

The variable I_{13} in equation (1) can be calculated by

$$I_{13} = \frac{\partial \varepsilon_\mathrm{v}}{\partial s} \tag{19}$$

Equation (19) denotes that I_{13} is a ratio of incremental volumetric strain to incremental suction when p and q are constant. This variable can describe shrinkage and swelling of unsaturated soils subjected to drying and wetting. Fig. 3 shows the experimental results of drying-induced shrinkage reported by Chiu and Ng [14]. The test soil was a compacted CDT, classified as a silt. Three different mean net stresses, 0, 40 and 80 kPa, were applied and maintained constant during the drying process. It is evident that the void ratio reduced nonlinearly with an increase in suction. More importantly, the reduction rate was affected by stress, suggesting that I_{13} is a function of stress.

To model the suction-induced volume changes of unsaturated soils, several formulations have been reported in the literature, as reviewed Sheng [80]. Among these formulations, the equation of Sheng et al. [81] consider of the influence of mean net stress on the shrinkage/swelling of unsaturated soils. It is used to show the interpretations of suction-induced volume change in the unified framework (i.e., equation (1)):

$$de = \frac{\alpha_s ds}{p+s} \tag{20}$$

where α_s is the compressibility of unsaturated soils upon a change in suction. The value of α_s strongly depends on the suction history, which governs the location of yield surface. Four different cases are considered: (1) When the soil is subjected to drying and the current suction is equal to the maximum suction in the suction history (i.e., on the yield surface), α_s is equal to the shrinkage index λ_s; (2) when the soil is subjected to drying but the current suction is below the maximum suction in the suction history (i.e., within the yield surface), α_s is equal to the swelling index κ_s; (3) when the soil is subjected to wetting and the soil is over-consolidated (i.e., soil state within the yield surface), α_s is equal to the swelling index κ_s; and (4) when the soil is subjected to wetting and the soil is normally consolidated (i.e., soil state on the yield surface), wetting collapse occurs and α_s is equal to the accumulation rate of plastic strain.

Based on equations (19) and (20), the following equation can be derived:

$$I_{13} = \frac{\lambda_s}{(1+e)(p+s)} \tag{21}$$

A key feature of equation (20) is that the suction-induced volume changes of unsaturated soils are dependent on mean net stress. The coupling effects of hydromechanical behaviour are taken into account.

2.4 Determination of the variable I_{21}

The variable I_{21} in equation (1) can be determined using the following equation:

$$I_{21} = \frac{\partial \varepsilon_q}{\partial p} \tag{22}$$

According to equation (22), the variable I_{21} is the ratio of incremental deviator strain to incremental mean net stress when q and s are constant. Moreover, the incremental deviator strain can be calculated using

$$d\varepsilon_q = \frac{d\varepsilon_v - \kappa(s) dp/p}{D_p} \tag{23}$$

where D_p is the dilatancy associated with the plastic mechanism of compression. D_p of unsaturated soils has been studied previously through compression tests under constant ratio of suction to stress. Fig. 4 shows the experimental results of D_p of a compacted silt at the suctions of 200, 400, 600 and 1500 kPa [18]. During the compression process, the stress ratio was maintained at 1. D_p was clearly affected by soil suction, particularly at mean net stresses below 300 kPa. To model the suction-dependent D_p, Chiu and Ng [15] proposed the following equation:

$$D_{\mathrm{p}} = \big(\lambda(\mathrm{s}) - \kappa(\mathrm{s})\big) d_2(\mathrm{s}) \frac{M}{\eta} \tag{24}$$

Based on equations (22) through (24), the following equation can be derived:

$$I_{21} = \frac{I_{11} - \kappa(\mathrm{s})/p}{\big(\lambda(\mathrm{s}) - \kappa(\mathrm{s})\big) d_2(\mathrm{s}) M/\eta} \tag{25}$$

It can be seen that the value of I_{21} is affected by suction. Therefore, the state-dependent dilatancy of unsaturated soils is considered by equation (25) and hence by equation (1).

2.5 Determination of the variable I_{22}

The variable I_{22} in equation (1) can be determined using

$$I_{22} = \frac{\partial \varepsilon_{\mathrm{q}}}{\partial q} \tag{26}$$

According to equation (26), I_{22} is the ratio of incremental deviator strain to incremental deviator stress when p and s are constant. This variable is closely related to the tangent shear modulus G (i.e., $I_{22} = 1/G$), which has been studied by many researchers [3, 16]. It is well recognised that G of soil depends one strain, as shown in Fig. 5. At very small strains below 0.001%, shear modulus is almost constant and it is denoted by G_0. The value is widely used for different purposes, such as the calculation of ground movement under dynamic loads. At small strains between 0.001 to 0.01%, shear modulus reduces significantly with an increase in strain. At the working condition of many civil engineering structures in relatively medium and dense/stiff soils, typical strains encountered fall within the small strain range [4, 50, 65]. In this following section, the formulation of G_0 and the strain-dependence of shear modulus are discussed. A formulation for I_{22} is then derived.

2.5.1 Initial shear modulus G_0 at very small strains

Through a series of resonant column tests on unsaturated sand, Wu et al. [96] found that as the degree of saturation increased, G_0 first increased and then decreased. The maximum value occurred at a degree of saturation of about 20%. A similar relationship between G_0 and the degree of saturation was observed by Qian et al. [74]. In these two studies, soil suction was not controlled/measured and soil specimens were compacted at different water contents, resulting in different soil microstructures and hence these specimens could not be qualified as 'identical' [57]. In more recent studies, soil specimens were generally prepared at the same water content and density to obtain the same microstructure. After preparation, the soil specimens were subjected to drying and wetting in suction-controlled apparatus prior to the determination of G_0. Using a suction-controlled resonant column, Mancuso et al. [51] investigated G_0 of a compacted silty sand subjected to isotropic compression at constant suction. They found that G_0 increased with suction. Similar findings from different unsaturated soils have also been reported by many researchers [36, 64, 78, 89]. Apart from suction, the effects of suction history on anisotropic G_0 were identified by Ng et al. [63], as shown in Fig. 6. They applied a drying and wetting cycle to unsaturated silt at constant net stress. It was found that at the same suction, G_0 was higher along the wetting path than along the drying path. They revealed that apart from the current suction, the suction path also affected the stiffness of unsaturated soils. Their finding was confirmed by Khosravi and Mccartney [41] who tested another compacted silt.

Some semi-empirical equations have been reported in the literature to describe G_0 of unsaturated soil. In this review, these equations are classified into four types based on their constitutive variables. The first type of G_0 models, such as equations (B1) through (B3) in Table 3, adopts net stress suction as constitutive variables. One example is equation (B1) proposed by Leong et al. [43]. This equation considered the influence of stress and suction, but it ignored the influence of stress path and suction path. As a consequence, effects of degree of saturation and density on G_0 cannot be captured. More importantly, this equation is only applicable for isotropic condition, including isotropic soil fabric and isotropic stress state. Ng and Yung [64] proposed equation (B2) to describe the anisotropic G_0 of unsaturated soil. According to equation (B2), the anisotropic G_0 of unsaturated soils is affected by the soil fabric, void ratio, stress and suction. In addition, Sawangsuriya et al. [78] proposed equation (B3) for the G_0 of unsaturated soil. Different from equations (B1) and (B2), this equation uses multiplication rather than addition. Hence, suction-induced variation of G_0 is independent of stress in equation (B3). In other words, the effects of stress and suction on G_0 are assumed to be independent. On the other hand, it should be pointed out that the first type of G_0 models predicts a unique relationship between G_0 and suction when stress and void ratio are constant. Effects of suction history are not captured by the first type of G_0 models. To improve these models, a possible approach is to incorporate degree of saturation or water content.

The second type of G_0 models, such as equations (B4) and (B5) in Table 3, is based on effective stress of unsaturated soil. In equation (A4) proposed by Sawangsuriya et al. [78], the effective stress of unsaturated soil is taken as $(\sigma - u_a)+S_r^{\kappa}(u_a - u_w)$. The typical values of parameter κ were found to range from 1 to 3. At a given suction, the calculated G_0 is therefore smaller along the wetting path than that along the drying path. This predicted tread is different from experimental results reported by many researchers (see Fig. 6). Recently, Pagano et al. [72] developed a microscale-based model (i.e., equation (A5)) for G_0 in unsaturated granular geomaterials. In their formulation, σ_i is the intergranular stress of the unsaturated packing; σ_i^b and σ_i^m are the intergranular stresses in the regions of bulk water and meniscus water, respectively. It is conceptually good to differentiate intergranular stresses in bulk water and meniscus water, considering these two types water are very different in changing intergranular stresses [92]. This microscopic approach, however, leads to great difficulty in model calibration.

To properly consider the effects of suction history on G_0, some recent models used two constitutive variables, at least one of which is a function of degree of saturation. Equations (B6) through (B9) in Table 3 all belong to this type of G_0 model [7, 41, 95]. Equation (B6), which was proposed by Sawangsuriya et al. [78], has six model parameters (A, K, b, n, λ and κ). A lot of test results are required to calibrate all of these parameters. Similarly, equation (A7) [7] requires the information of NCLs to compute OCR of a soil, apart from five models parameters (A, n, m, a and b). Wong et al. [95] developed a semi-empirical equation based on the effective stress formulation of Khalili and Khabbaz [40]. Compared with the model of Biglari et al. [7], the model of Wong et al. [95] adopts a void ratio function to consider effects of stress history, instead of incorporating both OCR and void ratio. Consequently, less model parameters are required in the model of Wong et al. [95]. Wong et al. [95] applied the three above models to predict G_0 of different soils along various stress paths. They found that along the drying and isotropic compression processes, the predictions using these three models are quite consistent with measured data. Furthermore, equations of Biglari et al. [7] and Wong et al. [95] are able to capture the variation of G_0 along cycles of drying and wetting. Dong et al. [20] proposed the G_0 model based on effective stress and effective degree of saturation. This model is qualitatively similar to that of Wong et al. [95].

The last type of G_0 models includes equations (B10) through (B12) in Table 3. These models use a reference G_0 at a specific moisture condition (generally the fully saturated or completely dry condition), and calculate the variation of G_0 with soil moisture. Hence, these models do not require an explicit consideration of stress state variables. Equation (A10), which was proposed by Wu et al. [96], used the function $H(S_r)$ to calculate the variation of G_0 with soil moisture condition. Mancuso et al. [51] proposed equation (B11), in which parameter β controls the increase rate of G_0 with increasing suction; r is the ratio of shear modulus at a very high suction and $(G_0)_{s*}$. Han and Vanapalli [34] proposed equation (B12) to calculate the variation of G_0 with increasing suction and degree of saturation. To improve the model prediction, two reference values of G_0 are used, including the fully saturated state and an unsaturated state. This type of models is simple, but they may not be able to capture some important aspects of soil stiffness. For example, by using a scalar (water content/degree of saturation), suction effects on stiffness anisotropy (see Fig. 6) cannot be simulated. In addition, the hysteresis of stiffness during drying and wetting cannot be captured.

As discussed above, theoretical formulations for G_0 in Table 3 may be classified into four types based on the constitutive stress variables. One equation from each type, including equations (B2), (B4), (B9) and (B12), is selected to simulate the very small strain behaviour of an unsaturated silt. The very small strain moduli G_0 of this soil were measured by Ng and Yung [64] and Ng et al. [63] along two different stress paths, including constant-s compression and constant-p drying and wetting. The measured and calculated results are compared in Fig. 7 and parameter values are shown in Table 4. To evaluate the performance of each equation, the coefficient of determination (R^2) is calculated and shown in the figure. During the constant-s compression, equation (B2) [64] gives the best prediction of G_0, with R^2 values of 0.97. This is mainly because equation (B2) uses the two independent stress state variables. The increase rates of G_0 with increasing suction and stress can be well simulated using two independent terms: $\left[(\sigma_\mathrm{i}-u_\mathrm{a})/p_\mathrm{atm}\cdot(\sigma_\mathrm{j}-u_\mathrm{a})/p_\mathrm{atm}\right]^n$ and $(1+s/p_\mathrm{atm})^n$. When equation (B4) [78] is used, however, there is an obvious discrepancy between measured and calculated results with R^2 of 0.62. This problem is mainly because equation (B4) is based on a single constitutive stress variable, which is not sufficient to capture the influence of net stress, suction and degree of saturation in a unified formulation. During the constant-*p* drying and wetting, equation (B9) [20] gives the best prediction of experimental results (R^2 = 0.89). This is because this equation properly considers at least two different effects of suction path: (a) altering the suction stress and hence effective stress proposed [47]; (b) affecting suction hardening [38]. Equation (B12) [34] gives the lowest value of R^2 (i.e., 0.65). This is because at a given suction, the model predicts a higher G_0 along the drying path, while the experimental results reveal that G_0 is larger along the wetting path. In addition, equation (B2) [64] is not able to well capture the variation of G_0 during drying and wetting (R^2 = 0.67), because this equation does not include S_r. In addition, during the constant-*p* drying and wetting, the values of R^2 are less than 0.9 for all equations. Further studies are therefore required to improve the modelling of suction path on G_0.

2.5.2 Reduction in shear modulus with increasing strain

To determine the stiffness strain relationship of a Singapore residual soil (clayey sand), Leong et al. [43] carried out a series of undrained triaxial compression tests. Ten specimens with different suctions were sheared at constant water content and constant confining stress. They observed that the shear modulus increased consistently with initial suction and confining stress. It should be noted that suction was not controlled during the isotropic compression and shearing process, and the reported degradation of shear stiffness was a function of deviator strain as well as varying with suction during shearing. Ng and Xu [62] carried out a series of suction-controlled constant mean net stress shear tests to investigate the effects of suction on the small-strain behaviour of an unsaturated CDT. Suction was controlled using the axis-translation technique. After the specimens were equalised under the target mean net stress and target suction, they were sheared under constant mean net stress and constant suction. As shown in Fig. 8, the initial shear stiffness and stiffness degradation are affected by suction.

On the other hand, various semi-empirical equations have been proposed to model the degradation of shear modulus with strain based on experimental studies of saturated soils (see for example [71, 88, 99]). One example is the following hyperbolic equation proposed by Vardanega and Bolton [88]:

$$\frac{G}{G_0} = \begin{cases} 1 & for\ \varepsilon_q < \varepsilon_{qe} \\ \dfrac{1}{1+\left(\dfrac{\varepsilon_q - \varepsilon_{qe}}{\varepsilon_{qref} - \varepsilon_{qe}}\right)^{\alpha}} & for\ \varepsilon_q \geq \varepsilon_{qe} \end{cases} \tag{27}$$

where G is the secant shear modulus at any deviator strain; ε_q is deviator strain; α is a curvature parameter that controls the degradation rate of shear modulus with strain; and ε_{qe} is the elastic threshold strain beyond which shear modulus decreases with increasing deviator strain. ε_{qref} is a characteristic reference strain, defined as the deviator strain at which secant shear modulus is reduced to $0.5G_0$. Parameter α is mainly affected by the soil type, while ε_{qe} and ε_{qref} depends on not only the soil type but also the soil state (for example, the void ratio and stress level) [88]. Equation (27) was originally developed by Vardanega and Bolton [88] for saturated soils. Zhou [105] illustrated that it can be used for unsaturated soils with a minor modification. In unsaturated soil, meniscus water increases the inter-particle normal force, which would stabilise the soil skeleton. Hence, the elastic threshold strain (ε_{qe}) in equation (27) is expected to increase when soil becomes desaturated.

2.5.3 Formulation for I_{22}

According to equations (26) to (27), it can be shown that the value of I_{22} depends on the current deviator strain. When it is lower than the elastic threshold strain, shear modulus is constant. Hence,

$$I_{22} = \frac{1}{C^2 f(e)\left(\frac{p}{p_r}\right)^{2n}\left(1+\frac{s}{p_r}\right)^{2k}} \tag{28}$$

When the current deviator strain is above the elastic threshold value, the strain dependence of shear modulus should be considered. I_{22} is calculated using the following equation:

$$I_{22} = \frac{1+\left(\frac{\varepsilon_q - \varepsilon_{qe}}{\varepsilon_{qref} - \varepsilon_{qe}}\right)^{\alpha}}{C^2 f(e)\left(\frac{p}{p_r}\right)^{2n}\left(1+\frac{s}{p_r}\right)^{2k}} \tag{29}$$

There are four parameters in equations (28) and (29): C, n, k and α. The first three parameters can be obtained from stress and suction-controlled bender element and resonant column tests, while the last one can be determined through a constant-p shear test.

2.6 Determination of the variable I_{23}

According to equation (1), the variable I_{23} is equal to

$$I_{23} = \frac{\partial \varepsilon_{\mathrm{q}}}{\partial s} \tag{30}$$

Equation (30) suggests that I_{23} is the ratio of incremental/decremental deviator strain to incremental/decremental suction when p and q are constant. Hence, the value of I_{23} can be calibrated using stress-controlled drying/wetting tests. Fig. 9 shows the development of deviator strain of a compacted gravelly sand subjected to wetting [54]. This study considered four mean net stresses of 0, 50, 100 and 200 kPa, and applied a stress ratio of 1.4 in all tests. During the wetting process, the deviator strain accumulated at an increasing rate, because yielding had occurred when the wetting path reached the yield surface. Assuming that the wetting-induced deviator strain is essentially plastic (i.e., elastic strain is zero), the slope of deviator strain-suction relation is equal to I_{23}.

It should be pointed out that in most drying/wetting tests reported in the literature, only volumetric strain was measured under an assumption of isotropic soil behaviour. Hence, experimental results of suction-induced deviator strain are very limited. If suction-induced elastic deviator strain is small and can be ignored, equation (30) suggests

$$I_{23} = \frac{1}{D_{\mathrm{s}}} \frac{\partial \left[\varepsilon_{\mathrm{v}} - \frac{\kappa_{\mathrm{s}} \mathrm{d}s}{(p+s)(1+e)}\right]}{\partial s} \tag{31}$$

where D_{s} is the dilatancy during drying/wetting. D_{s} generally take the value of D_{q} and D_{p} (see equations (A3) and (15)), when suction-induced yielding occurs for the plastic mechanisms of shearing and compression, respectively. Based on equations (20) and (31), the following equation is derived:

$$I_{23} = \frac{I_{13}}{D_{\mathrm{s}}} - \frac{\alpha_{\mathrm{s}}}{D_{\mathrm{s}}(p+s)(1+e)} \tag{32}$$

Equation (32) implies that I_{23} is a function of I_{13}, α_{s} and D_{s}, which can be all determined based on experimental results, as introduced and discussed previously. Hence, the value of I_{23} can be readily calculated in this alternative approach. No extra tests are required for calibrating I_{23}.

2.7 Determination of the variable I_{31}

The variable I_{31} in equation (1) can be determined by

$$I_{31} = \frac{\partial S_{\mathrm{r}}}{\partial p} \tag{33}$$

According to equation (33), the variable I_{31} is the ratio of the incremental degree of saturation to incremental mean net stress when q and s are constant. Hence, this variable is closely related to the stress-dependent SWRC of unsaturated soils. The following paragraphs first discuss the measurement and modelling of a SWRC. Then, a specific SWRC model is used as an example to derive a formulation for I_{31}.

2.7.1 Stress-dependence of the SWRC

Various experimental technologies have been developed for determining the SWRC in soil science and agriculture-related disciplines, such as the Tempe pressure cell, the volumetric pressure plate extractor, the pressure membrane extractor and the osmotic desiccator [22]. However, these apparatuses do not take into account of the deformation and stress of soil as well as their influence on the SWRC. It is implicitly assumed that the SWRC of a given soil is unique. As a consequence, the value of I_{31} is assumed to be zero.

Different from soil science and agriculture-related disciplines, in geotechnical engineering the soil state including the density and stress is an important variable. This is because soil behaviour depends strongly on the soil state. Since about 20 years ago, the influence of soil density and deformation on SWRC has been recognised and actively investigated. Although the net stress of soil specimen was not controlled in their study, Vanapalli et al. [87] tested several specimens with different initial void ratios. With a reduction in the void ratio from 0.59 to 0.54, the water retention ability of soil was greatly improved, particularly at suctions lower than 100 MPa. A further reduction in the void ratio from 0.54 to 0.51 did not affect the water retention ability too much. The influence of the initial density on the SWRC has been reported by a large number of researchers [58, 85]. The observed effects of soil density on the SWRC are attributed to the fact that the average pore size of a soil specimen decreases as a result of deformation. The influence of pore size distribution on a SWRC cannot be known and modelled explicitly.

Ng and Pang [59] developed a new stress-controllable pressure plate apparatus, which can be used to determine the SWRC of unsaturated soils subjected to different stress states. Using the modified apparatus, the researchers measured the SWRC of unsaturated silt at vertical net stresses of 0, 40 and 80 kPa. The results are shown in Fig. 10. It is clear that the SWRC was greatly affected by stress. The water retention ability of the soil specimens increased with stress. Similar observation was reported by Lee et al. [42] and their results is shown in Fig. 11. The effects of stress on the SWRC were partially due to the average density-dependence of the SWRC. As reported by Vanapalli et al. [87], when stress increases, the density increases and so does the water retention ability. It should be pointed out that, however, stress effects are not equivalent to density effects. This is because the application of stress affects not only soil density (or void ratio) but also pore size distribution, as illustrated by the results of MIP tests shown in Fig. 12.

2.7.2 Modelling the stress-dependent SWRC

Many SWRC models have been reported in the literature, and they may be classified into three types. The major difference comes from their approaches for considering the influence of soil state on the SWRC. The first type of SWRC models adopts a unique relationship between suction and soil moisture. Examples include equations (C1) through (C3) in Table 5 [23, 30, 86]. The SWRC calculated using these models is a curve in the S_r-s plane. Even though these models are widely used in practice for simplicity, they do not consider the coupling effects between the hydraulic and mechanical behaviour of unsaturated soils. Due to this limitation, I_{31} predicted by these equations is always regarded as zero.

The second type of SWRC models explicitly considers effects of soil density on the water retention behaviour of unsaturated soil, such as equations (C4) and (C6) in Table 5. Among these models, Gallipoli et al. [27] employed a closed-form equation which was modified from the Van Genuchten [86] model by including the void ratio (e) in the formulation. Hence, S_r is a function of not only suction but also the void ratio. The calculated SWRC becomes as a surface in the S_r-s-e space. Tarantino [85] modified the model of Gallipoli et al. [27] by reducing one parameter based on extensive tests on both fine-grained and coarse-grained soils. Experimental results revealed that the product of S_r and e is almost independent of e at high suction. Based on this experimental evidence, it can be derived that the product of $m_1 m_2 m_4$ should be equal to 1. Sheng and Zhou [83] proposed an incremental form. The influence of void ratio on the SWRC was taken into account. This type of models implicitly assumes that stress effects are equivalent to density effects on the SWRC.

The last type of SWRC model (denoted as equation (C7) in Table 5) was proposed by Zhou and Ng [106]. Equation (C7) was developed from the following equation.

$$S_{\mathrm{r}} = \left[1 + \left(s \frac{e^{m_4}}{m_3} \left(\frac{\xi_{\mathrm{m}}}{\xi_{\mathrm{m}}^{\mathrm{ref}}}\right)^{-m_{\mathrm{m}}}\right)^{m_2}\right]^{-m_1} \tag{34}$$

where ξ_m is the ratio between the volume of micro-pores (V_M) to the total volume of pores (V_T) which characterises the pore size distribution (PSD), ξ_0 is the initial value of ξ_m before applying any net stress; and m_1, m_2, m_3, m_4 and m_m are model parameters. This model takes into account two different effects of net stress on the SWRC: stress-induced change in the average void ratio and stress effects on the pore size distribution. The first effect is described by the following equation:

$$e = e_0 - \alpha_{\mathrm{p}} \, ln\left(1 + \frac{p}{p_{\mathrm{atm}}}\right) - \alpha_{\mathrm{s}} \, ln\left(1 + \frac{s}{p_{\mathrm{atm}}}\right) \tag{35}$$

Moreover, the following equation was derived for the theoretical relationship between PSD parameters and net mean stress:

$$\zeta_{\mathrm{m}} = \zeta_{\mathrm{m}}^{\mathrm{ref}} \left(1 + \frac{p}{p_{\mathrm{atm}}}\right)^{-m_5} \quad (36)$$

Equation (36) determines the relationship between the proportion of macro-pores and net stress. Hence, the influence of stress on the pore size distribution is considered in a simplified manner. By considering the net stress effects on water retention ability, the new constitutive relation can overcome the limitations of previous studies based on soil science.

The performance of three SWRC models is evaluated here, including equation (C2) [86], equation (C5) [85] and equation (C7) [106]. Equation (C2) assumes a rigid soil and equations (C5) and (C7) are derived from this equation by considering density effects and stress effects, respectively. These three equations are representative of most SWRC models in Table 5, as discussed above. They are used to simulate the experimental results of Ng and Pang [59] and Lee et al. [42]. Ng and Pang [59] carried out two series of tests to investigate the influence of density and vertical stress on the water retention behaviour of a clayey silt. In the first series of tests, three specimens with different initial void ratios of 0.86, 0.75 and 0.69 were dried at zero net stress. In the second series of tests, three specimens with the same initial void ratio (0.69) were dried at different vertical net stresses of 0, 40 and 80 kPa. Lee et al. [42] measured WRCs of a silty sand at various stresses, similar to the second series of tests in Ng and Pang [59]. The measured and calculated SWRCs are shown in Fig. 10 and Fig. 11. Parameter values are summarized in Table 6. It is revealed from the comparisons that:

(a). Among the three equations, equation (C7) show the best performance, with R^2 above 0.97 in all cases (see Fig. 10(e), Fig. 10(f) and Fig. 11(c)). This equation is able to well capture density effects and stress effects observed in both studies. It should be noted that even though equation (C7) gives the best prediction of the above experimental results, it considers stress effects on pore structure in a simplified approach. The ratio of inter-aggregate pore volume to intra-aggregate pore volume is used to describe pore structure. This ratio does not account for some features of pore structure, such as the pore size distribution, pore orientation, pore connection and pore shape. Other stress-dependent SWRC models in the literature have similar simplifications [76]. More studies are required to better understand stress effects on the pore structure and hence SWRC of unsaturated soil.

(b). Equation (C5) gives the same prediction as equation (C7) for density effects ((see Fig. 10(c) and Fig. 10(e)), because equation (C7) reduces to this equation when net stress is zero. Equation (C5), however, slightly underestimate stress effects on SWRC (R^2 = 0.95 and 0.94 in Fig. 10(d) and Fig. 11(b), respectively). This deficiency is caused by the limitation of equation (C5), which can only partially consider stress effects through the change in void ratio. In the past two decades, many SWRC models have been proposed with a consideration of soil deformation [28, 37, 73, 75, 85, 103], as summarized in Table 5. Even though they have been developed using different approaches, they all implicitly assume that stress effects are equivalent to density effects on the SWRC. Hence, they are expected to show similar performances as equation (C7). Their performance is lightly worse than equation (C7), but less parameters are required. This type of models may be used as an approximation if the stress change is not very significant.

(c). Equation (C2) only predicts a single SWRC for each soil at different test conditions (see Fig. 10(a), Fig. 10(b) and Fig. 11(a)), as expected. Even though this model is widely used in practice for simplicity, density effects and stress effects cannot be captured. It does not consider the coupling effects between the hydraulic and mechanical behaviour of unsaturated soils. Due to this limitation, I_{31} predicted by the equation is always zero. Other similar equations, such as equations (C1) through (C3) in Table 5 [23, 30, 86], have similar limitation. These models are expected to show similar performance as equation (C2).

Based on the discussion above, the SWRC model proposed by Zhou and Ng [106] shows a fundamental advantage in modelling stress-dependent the SWRC. Based on equations (33) to (36), the following equation can be derived:

$$I_{31} = \frac{\partial S_{\mathrm{r}}}{\partial e}\frac{\partial e}{\partial p} + \frac{\partial S_{\mathrm{r}}}{\partial \xi}\frac{\partial \xi}{\partial p} \tag{37}$$

Then,

$$I_{31} = \frac{\partial S_{\mathrm{r}}}{\partial e}(1+e)I_{11} + \frac{\partial S_{\mathrm{r}}}{\partial \xi}\frac{\partial \xi}{\partial p} \tag{38}$$

It should be noted that the first type of SWRC models (i.e., equations (C1) to (C3) in Table 5) assume that I_{31} is equal to zero, while the second type of SWRC models (i.e., equations (C4) to (C6) simply consider the first term on the right-hand of equation (38).

2.8 Determination of the variable I_{32}

The variable I_{32} in equation (1) can be determined using the following equation:

$$I_{32} = \frac{\partial S_{\mathrm{r}}}{\partial q} \tag{39}$$

According to equation (39), the variable I_{32} is the ratio of the incremental/decremental degree of saturation to incremental/decremental deviator stress when p and s are constant. Ideally, I_{32} is determined from the relationship between S_r and q based on shear tests at constant-p and s condition. Such data is very limited in the literature because it is uncommon to carry out constant-*p and s* shear tests. Alternatively, it can be determined using data from SWRCs at various q conditions. Ng et al. [56] measured the SWRCs of a compacted silt. Three different values of the stress ratio q/p (0, 0.75 and 1.2), corresponding to different deviator stresses, were applied. They found that the influence of deviator stress on the SWRC was much smaller than the effects of mean net stress. Based on this observation, mean net stress is directly incorporated in the SWRC model, while the effects of deviator stress on SWRC are described using void ratio for simplicity. Hence, equation (39) can be derived as follows:

$$I_{32} = \frac{\partial S_{\mathrm{r}}}{\partial e}\frac{\partial \varepsilon_{\mathrm{v}}}{\partial q}(1+e) \tag{40}$$

Based on equations (16), (39) and (40), the following equation can be derived:

$$I_{32} = \frac{\partial\left[1+\left(s\frac{e^{m_4}}{m_3}\left(\frac{\xi_{\mathrm{m}}}{\xi_{\mathrm{m}}^{\mathrm{ref}}}\right)^{-m_{\mathrm{m}}}\right)^{m_2}\right]^{-m_1}}{\partial e} D_{\mathrm{q}}(1+e)I_{22} \tag{41}$$

Equation (41) suggests that the value of I_{32} is affected by several factors, including density effects on the SWRC, D_{q} and I_{22}. A lot of data is available in the literature for determining each of them, so I_{32} can be determined based on experimental results readily.

2.9 Determination of the variable I_{33}

The variable I_{33} in equation (1) can be calculated using the following equation:

$$I_{33} = \frac{\partial S_r}{\partial s} \tag{42}$$

According to equation (42), the variable I_{33} is the ratio of the incremental degree of saturation to incremental suction when p and q are constant. This variable is related to desorption/adsorption rates of unsaturated soils. Based on equations (34) and (42), the following equation can be derived:

$$I_{33} = \frac{\partial\left[1+\left(s\frac{e^{m_4}}{m_3}\left(\frac{\xi_{\mathrm{m}}}{\xi_{\mathrm{m}}^{\mathrm{ref}}}\right)^{-m_{\mathrm{m}}}\right)^{m_2}\right]^{-m_1}}{\partial s} \tag{43}$$

It should be noted that the value of I_{33} is not constant, but dependent on suction and stress. Moreover, the influence of stress on I_{33} is related to change in the average void ratio and pore size distribution.

Apart from stress-dependence, hydraulic hysteresis also imposes great influence on the water retention behaviour of unsaturated soil. At a given suction, the equilibrium water content along the drying path is higher than or equal to that along the wetting path. So far, some theoretical models have been proposed for the hysteretic water retention behaviour of unsaturated soil. In each model with an assumption of rigid soil, two boundary curves are generally defined, including the main drying curve and main wetting curve. Any state in the S_{r}-s plane is bounded by these two curves. Similarly, a main drying surface and a main wetting surface are defined in the S_r-s-e space or S_r-s-p space, if density/stress effects on SWRC are considered in the model. When soil state is on the main drying and wetting curves/surfaces, S_r is simply calculated from s, e and p. When soil state is between the main drying and wetting curves/surfaces, S_r is affected by not only s and e but also suction path, due to the existence of hydraulic hysteresis. Different methods have been used in the theoretical model to simulate the scanning curves between the main drying and wetting curves/surfaces. Wheeler et al. [92] modelled the water retention behaviour in a classic elastoplastic framework. Two processes were defined, including the elastic and elastoplastic processes. During each process, a constant adsorption/desorption rate was assumed. Similar approaches were used in many unsaturated soil models [24, 70, 81, 94]. These approaches cannot predict a smooth transition between scanning curves and main curves/surfaces, since the adsorption/ desorption rate during the elastoplastic process is much larger than that during the elastic process. To solve this problem, Li [44] applied the bounding surface theory to model the hysteretic water retention behaviour of unsaturated soil. Different from the model of Wheeler et al. [92], the adsorption/desorption rate is not constant when soil state is between the main drying and wetting curves. The adsorption/desorption rate is affected by suction history, the current suction and degree of saturation. The model of Li [44] assumes a rigid soil, so density and stress effects on SWRC cannot be captured. In recent years, some advanced water retention models have been proposed with a consideration of density effects and hysteresis effects [25, 104, 108]. Zhou et al. [108] developed a bounding surface model with a consideration of the influence of soil deformation on water retention behaviour. The main drying/wetting curves in the model of Li [44] was extended from S_r-s plane to S_r-s-e space. Gallipoli et al. [25] proposed a new term (i.e., scaled suction s^*), which is a function of suction and void ratio. By adopting the scaled suction, the main drying/wetting surfaces in the S_r-s^* plane become as two curves. It should be pointed out that all the above models do not explicitly consider the reasons for hydraulic hysteresis. These models are therefore semi-empirical. Hence, some researchers attempt to model the hysteretic water retention behaviour with an explicit consideration of specific reasons for hydraulic hysteresis. For instance, Zhou [102] applied different contact angles for advancing and receding water meniscus, leading to different water retention abilities during the drying and wetting processes. Cheng et al. [13] incorporated the influence of pore non-uniformity on the water retention behaviour. These models have clear physical meaning, but the calibration of soil parameters is not very straightforward. More studies at the micro and macro levels are needed in the future.

2.10 Discussion on the simple and unified framework

Based on the discussion above, it is illustrated that I_{ij} (i = 1, 2 and 3; j = 1, 2 and 3) in equation (1) can be derived theoretically. More importantly, these nine variables can be calibrated from suction- and stress-controlled unsaturated soil tests. Hence, equation (1) provides a simple but effective framework for modelling the state-dependent behaviour of unsaturated soils.

It should be pointed out that equation (1) does not explicitly consider differentiate the elastic and elasto-plastic processes. To consider these two processes in numerical analysis, the variables I_{ij} (i = 1, 2 and 3; j = 1, 2 and 3) should take different values at different processes. For instance, in the formulation for I_{11} (i.e., equation (13)), $\alpha_p(s)$ is equal to $\kappa(s)$ and $\lambda(s)$ for the elastic process and elastoplastic process, respectively.

The cross terms in the compliance matrix of equation (1) are not independent. Firstly, I_{12} and I_{21} describe soil dilatancy during constant-p shearing and constant-q compression, respectively. Soil dilatancy during these two processes is modelled using a unified formulation in many constitutive models such as the Barcelona basic model (BBM) [1]. Secondly, I_{12} and I_{32} are closely related because shearing-induced volumetric strain (described by I_{12}) would affect the water retention behaviour (described by I_{32}) of unsaturated soil. Finally, I_{13} and I_{23} govern the volumetric and deviator strains induced by drying/wetting at a condition of constant p and q. The ratio of I_{13} and I_{23} represents soil dilatancy.

3 Conclusions

In this paper, the state-dependent hydro-mechanical behaviour of unsaturated soil is reviewed based on a unified and relatively simple framework. This framework uses mean net stress, deviator stress and suction as the constitutive stress variables. Theoretical models based on other constitutive stress variables can be also converted to this framework by matrix transformation. The nine variables, which have clear physical meanings, in the proposed compliance matrix are derived. Moreover, the calibration methods for these nine variables are discussed and explained.

Small strain stiffness of unsaturated soil is greatly affected by many factors, including strain, suction and suction path. So far, extensive formulations for G_0 at the very small strains (below 0.001%) can be found in the literature. Performance study of these formulations suggests that at least two constitutive stress variables are required to well capture the variation of G_0 along various stress paths, such as compression and drying/wetting. Moreover, most of the existing models cannot predict the hysteresis of stiffness during drying and wetting, because they have not incorporated effects of suction path properly. On the other hand, the modelling of stiffness degradation curve at small strains (between 0.001% and 1%) is relatively less studied. More unsaturated soil models for stiffness degradation are needed. Some other topics may also need further studies, including suction-induced anisotropy, effects of recent suction path.

Dilatancy of unsaturated soil is affected by not only stress ratio and density, but also some other factors such as suction and its path. With an increase in suction, soil dilatancy generally increases. It is therefore essential to model state-dependent dilatancy, which has not been incorporated in most of existing models. To model state-dependent dilatancy, the choice of void ratio function is not neutral. Based on test results analysed in this study, the use of (e-e_c) seems better than e/e_c, where e and e_c are the current void ratio and void ratio at critical state respectively. Furthermore, as far as the authors are aware, none of the existing model can capture the influence of drying and wetting cycles on the dilatancy of unsaturated soil. Effects of suction path on dilatancy needs further experimental and theoretical studies.

Stress effects and density effects on SWRC are fundamentally different. This is because net stress not only reduces average void ratio, but more importantly, alters the pore structure of unsaturated soil. The use of average void ratio to describe stress effects on water retention capability is therefore not sufficient. Hence, SWRC models including stress effects on pore structures are desired. More studies are required to better understand stress effects on the pore structure and hence SWRC of unsaturated soil.

Acknowledgement

The authors would like to thank the Research Grants Council (RGC) of the Hong Kong Special Administrative Region, China for providing financial support through the grants 16204817 and AoE/E-603/18.

References

1. Alonso EE, Gens A, Josa A (1990) A constitutive model for partially saturated soils. Géotechnique 40(3):405-430
2. Alonso EE, Iturralde EFO, Romero EE (2007) Dilatancy of coarse granular aggregates. Experimental unsaturated soil mechanics, Springer:119-135
3. Atkinson JH (2000) Non-linear soil stiffness in routine design. Géotechnique 50(5):487-507
4. Atkinson JH, Sallfors G (1991) Experimental determination of stress-strain-time characteristics in laboratory and in situ tests. Proceedings of the 10th European Conference on Soil Mechanics and Foundation Engineering, Florence, Italy 3:915-956
5. Bardet J-P (1986) Bounding surface plasticity model for sands. Journal of engineering mechanics 112(11):1198-1217

6. Been K, Jefferies MG (1985) A state parameter for sands. Géotechnique 35(2):99-112
7. Biglari M, Mancuso C, D'onofrio A, Jafari MK, Shafiee A (2011) Modelling the initial shear stiffness of unsaturated soils as a function of the coupled effects of the void ratio and the degree of saturation. Computers and Geotechnics 38(5):709-720
8. Bishop AW, Donald IB (1961) The experimental study of partly saturated soil in the triaxial apparatus. In: Proceedings of the 5th international conference on soil mechanics and foundation engineering, Paris. p 13-21
9. Chávez C, Alonso EE (2003) A constitutive model for crushed granular aggregates which includes suction effects. Soils and Foundations 43(4):215-227
10. Chen R (2007) Experimental study and constitutive modelling of stress-dependent coupled hydraulic hysteresis and mechanical behaviour of an unsaturated soil. PhD thesis, Hong Kong University of Science and Technology
11. Chen R, Ge Y, Chen Z, Liu J, Zhao Y, Li Z (2019) Analytical solution for one-dimensional contaminant diffusion through unsaturated soils beneath geomembrane. Journal of hydrology 568:260-274
12. Chen R, Xu T, Lei W, Zhao Y, Qiao J (2018) Impact of multiple drying–wetting cycles on shear behaviour of an unsaturated compacted clay. Environmental Earth Sciences 77(19):683
13. Cheng Q, Ng CWW, Zhou C, Tang CS (2019) A new water retention model that considers pore non-uniformity and evolution of pore size distribution. Bulletin of Engineering Geology and the Environment
14. Chiu CF, Ng CWW (2012) Coupled water retention and shrinkage properties of a compacted silt under isotropic and deviatoric stress paths. Canadian Geotechnical Journal 49(8):928-938
15. Chiu CF, Ng CWW (2003) A state-dependent elasto-plastic model for saturated and unsaturated soils. Géotechnique 53(9):809-829
16. Clayton CRI (2011) Stiffness at small strain: research and practice. Géotechnique 61(1):5-37
17. Croney D (1952) Suction of moisture held in soil and other porous materials.
18. Cui YJ, Delage P (1996) Yielding and plastic behaviour of an unsaturated compacted silt. Géotechnique 46(2):291-311
19. D'onza F, Gallipoli D, Wheeler SJ, Casini F, Vaunat J, Khalili N, Laloui L, Mancuso C, Masin D, Nuth M, Pereira JM, Vassallo R (2011) Benchmark of constitutive models for unsaturated soils. Géotechnique 61(4):283-302
20. Dong Y, Lu N, Mccartney JS (2016) Unified Model for Small-Strain Shear Modulus of Variably Saturated Soil. Journal of Geotechnical and Geoenvironmental Engineering:04016039

21. Duan X, Zeng L, Sun X (2019) Generalized stress framework for unsaturated soil: demonstration and discussion. Acta Geotechnica 14(5):1459-1481
22. Fredlund DG, Rahardjo H (1993) Soil mechanics for unsaturated soils. Wiley-interscience
23. Fredlund DG, Xing A (1994) Equations for the soil-water characteristic curve. Canadian Geotechnical Journal 31(4):521-532
24. Gallipoli D (2012) A hysteretic soil-water retention model accounting for cyclic variations of suction and void ratio. Géotechnique 62(7):605-616
25. Gallipoli D, Bruno AW, D'onza F, Mancuso C (2015) A bounding surface hysteretic water retention model for deformable soils. Géotechnique 65(10):793-804
26. Gallipoli D, Gens A, Sharma R, Vaunat J (2003) An elasto-plastic model for unsaturated soil incorporating the effects of suction and degree of saturation on mechanical behaviour. Géotechnique 53(1):123-135
27. Gallipoli D, Wheeler SJ, Karstunen M (2003) Modelling the variation of degree of saturation in a deformable unsaturated soil. Géotechnique 53(1):105-112
28. Gao Y, Sun DA (2017) Soil-water retention behavior of compacted soil with different densities over a wide suction range and its prediction. Computers and Geotechnics 91:17-26
29. Gao Y, Sun DA, Zhu Z, Xu Y (2019) Hydromechanical behavior of unsaturated soil with different initial densities over a wide suction range. Acta Geotechnica 14(2):417-428
30. Gardner W (1956) Mathematics of isothermal water conduction in unsaturated soils. Highway research board special report 40:78-87
31. Gens A, Potts DM (1982) A theoretical model for describing the behavior of soil not obeying Rendulic's principle. In: Int. Symp. on Numerical Models in Geomechanics. Balkema (ed.)
32. Gens A, Sánchez M, Sheng D (2006) On constitutive modelling of unsaturated soils. Acta Geotechnica 1(3):137
33. Goh S, Rahardjo H, Leong E (2014) Shear strength of unsaturated soils under multiple drying-wetting cycles. Journal of Geotechnical and Geoenvironmental Engineering 140(2):06013001
34. Han Z, Vanapalli SK (2016) Stiffness and shear strength of unsaturated soils in relation to soil-water characteristic curve. Géotechnique 66(8):627-647
35. Hilf JW (1956) An investigation of pore water pressure in compacted cohesive soils. Technical Memo 654, Denver: US Bureau of Reclamation
36. Hoyos LR, Suescún-Florez EA, Puppala AJ (2015) Stiffness of intermediate unsaturated soil from

simultaneous suction-controlled resonant column and bender element testing. Engineering Geology 188:10-28

37. Hu R, Chen YF, Liu HH, Zhou CB (2013) A water retention curve and unsaturated hydraulic conductivity model for deformable soils: consideration of the change in pore-size distribution. Geotechnique 63(16):1389-1405
38. Khalili N, Geiser F, Blight G (2004) Effective stress in unsaturated soils: Review with new evidence. International journal of Geomechanics 4(2):115-126
39. Khalili N, Habte M, Zargarbashi S (2008) A fully coupled flow deformation model for cyclic analysis of unsaturated soils including hydraulic and mechanical hystereses. Computers and Geotechnics 35(6):872-889
40. Khalili N, Khabbaz MH (1998) A unique relationship for chi for the determination of the shear strength of unsaturated soils. Geotechnique 48(5):681-687
41. Khosravi A, Mccartney JS (2012) Impact of Hydraulic Hysteresis on the Small-Strain Shear Modulus of Low Plasticity Soils. Journal of Geotechnical and Geoenvironmental Engineering, ASCE 138(11):1326-1333
42. Lee IM, Sung SG, Cho GC (2005) Effect of stress state on the unsaturated shear strength of a weathered granite. Canadian Geotechnical Journal 42(2):624-631
43. Leong EC, Cahyadi J, Rahardjo H (2006) Stiffness of a compacted residual soil. In: Unsaturated Soils 2006. p 1169-1180
44. Li XS (2005) Modelling of hysteresis response for arbitrary wetting/drying paths. Computers and Geotechnics 32(2):133-137
45. Li XS, Dafalias YF (2000) Dilatancy for cohesionless soils. Géotechnique 50(4):449-460
46. Lloret-Cabot M, Wheeler SJ, Pineda JA, Romero E, Sheng D (2018) From saturated to unsaturated conditions and vice versa. Acta Geotechnica 13(1):15-37
47. Lu N, Godt JW, Wu DT (2010) A closed‐form equation for effective stress in unsaturated soil. Water Resources Research 46(5)
48. Lu N, Likos WJ (2006) Suction stress characteristic curve for unsaturated soil. Journal of geotechnical and geoenvironmental engineering 132(2):131-142
49. Luo T, Chen D, Yao Y-P, Zhou A-N (2020) An advanced UH model for unsaturated soils. Acta Geotechnica 15(1):145-164
50. Mair RJ (1993) Unwin Memorial Lecture 1992 Developments in Geotechnical Engineering Research - Application to Tunnels and Deep Excavations. P I Civil Eng-Civ En 97(1):27-41

51. Mancuso C, Vassallo R, D'onofrio A (2002) Small strain behavior of a silty sand in controlled-suction resonant column torsional shear tests. Canadian Geotechnical Journal 39(1):22-31

52. Morvan M, Wong H, Branque D (2010) An unsaturated soil model with minimal number of parameters based on bounding surface plasticity. international journal for numerical and analytical methods in geomechanics 34(14):1512-1537

53. Ng CWW, Chiu CF (2001) Behavior of a loosely compacted unsaturated volcanic soil. Journal of Geotechnical Geoenvironmental Engineering, ASCE 127(12):1027-1036

54. Ng CWW, Chiu CF (2003) Laboratory study of loose saturated and unsaturated decomposed granitic soil. Journal of Geotechnical Geoenvironmental Engineering, ASCE 129(6):550-559

55. Ng CWW, Cui YJ, Chen R, Delage P (2007) The axis-translation and osmotic techniques in shear testing of unsaturated soils: A comparison. Soils and Foundations 47(4):675-684

56. Ng CWW, Lai CH, Chiu CF (2012) A modified triaxial apparatus for measuring the stress path-dependent water retention curve. Geotechnical Testing Journal, ASTM 35(3):490-495

57. Ng CWW, Menzies BK (2007) Advanced unsaturated soil mechanics and engineering. Taylor & Francis, London and New York

58. Ng CWW, Pang YW (2000) Experimental investigations of the soil-water characteristics of a volcanic soil. Canadian Geotechnical Journal 37(6):1252-1264

59. Ng CWW, Pang YW (2000) Influence of stress state on soil-water characteristics and slope stability. Journal of Geotechnical and Geoenvironmental Engineering, ASCE 126(2):157-166

60. Ng CWW, Sadeghi H, Hossen SB, Chiu CF, Alonso EE, Baghbanrezvan S (2016) Water retention and volumetric characteristics of intact and re-compacted loess. Canadian Geotechnical Journal 53(8):1258-1269

61. Ng CWW, Sadeghi H, Jafarzadeh F, Sadeghi M, Zhou C, Baghbanrezvan S (2020) Effect of microstructure on shear strength and dilatancy of unsaturated loess at high suctions. Canadian Geotechnical Journal 57(2):221-235

62. Ng CWW, Xu J (2012) Effects of current suction ratio and recent suction history on small-strain behaviour of an unsaturated soil. Canadian Geotechnical Journal 49(2):226-243

63. Ng CWW, Xu J, Yung SY (2009) Effects of wetting-drying and stress ratio on anisotropic stiffness of an unsaturated soil at very small strains. Canadian Geotechnical Journal 46(9):1062-1076

64. Ng CWW, Yung SY (2008) Determination of the anisotropic shear stiffness of an unsaturated decomposed soil. Géotechnique 58(1):23-35

65. Ng CWW, Zheng G, Ni J, Zhou C (2020) Use of unsaturated small-strain soil stiffness to the design of wall deflection and ground movement adjacent to deep excavation. Computers and Geotechnics 119:103375

66. Ng CWW, Zhou C (2014) Cyclic behaviour of an unsaturated silt at various suctions and temperatures. Géotechnique 64(9):709-720

67. Ng CWW, Zhou C, Leung AK (2015) Comparisons of different suction control techniques by water retention curves: Theoretical and experimental studies. Vadose Zone Journal 14(9):vzj2015.2001.0006

68. Ng CWW, Zhou C, Yuan Q, Xu J (2013) Resilient modulus of unsaturated subgrade soil: Experimental and theoretical investigations. Canadian Geotechnical Journal 50(2):223-232

69. Ng CWW, Zhou RZB (2005) Effects of soil suction on dilatancy of an unsaturated soil. In: Proceedings of the international conference on soil mechanics and geotechnical engineering. Aa Balkema publishers, p 559

70. Nuth M, Laloui L (2008) Advances in modelling hysteretic water retention curve in deformable soils. Computers and Geotechnics 35(6):835-844

71. Oztoprak S, Bolton MD (2013) Stiffness of sands through a laboratory test database. Géotechnique 63(1):54-70

72. Pagano AG, Tarantino A, Magnanimo V (2018) A microscale-based model for small-strain stiffness in unsaturated granular geomaterials. Géotechnique:1-14

73. Pasha AY, Khoshghalb A, Khalili N (2017) Hysteretic model for the evolution of water retention curve with void ratio. Journal of engineering mechanics 143(7):04017030

74. Qian X, Gray DH, Woods RD (1993) Voids and granulometry: effects on shear modulus of unsaturated sands. Journal of Geotechnical Engineering 119(2):295-314

75. Rojas E, Chávez O, Arroyo H, López-Lara T, Hernández J, Horta J (2017) Modeling the Dependency of Soil-Water Retention Curve on Volumetric Deformation. International Journal of Geomechanics 17(1):04016039

76. Roy S, Rajesh S (2020) Simplified Model to Predict Features of Soil–Water Retention Curve Accounting for Stress State Conditions. International Journal of Geomechanics 20(3):04019191

77. Russell A, Khalili N (2006) A unified bounding surface plasticity model for unsaturated soils. International Journal for Numerical and Analytical Methods in Geomechanics 30(3):181-212

78. Sawangsuriya A, Edil TB, Bosscher PJ (2009) Modulus-suction-moisture relationship for compacted soils in postcompaction state. Journal of Geotechnical and Geoenvironmental Engineering, ASCE 135(10):1390-1403

79. Sheng D, Sloan SW, Gens A (2004) A constitutive model for unsaturated soils: thermomechanical and

computational aspects. Computational Mechanics 33(6):453-465

80. Sheng DC (2011) Review of fundamental principles in modelling unsaturated soil behaviour. Computers and Geotechnics 38(6):757-776
81. Sheng DC, Fredlund DG, Gens A (2008) A new modelling approach for unsaturated soils using independent stress variables. Canadian Geotechnical Journal 45(4):511-534
82. Sheng DC, Gens A, Fredlund DG, Sloan SW (2008) Unsaturated soils: From constitutive modelling to numerical algorithms. Computers and Geotechnics 35(6):810-824
83. Sheng DC, Zhou AN (2011) Coupling hydraulic with mechanical models for unsaturated soils. Canadian Geotechnical Journal 48(5):826-840
84. Sun DA, Sheng DC, Sloan SW (2007) Elastoplastic modelling of hydraulic and stress–strain behaviour of unsaturated soils. Mechanics of Materials 39(3):212-221
85. Tarantino A (2009) A water retention model for deformable soils. Géotechnique 59(9):751-762
86. Van Genuchten MT (1980) A closed-form equation for predicting the hydraulic conductivity of unsaturated soils. Soil Science Society of America journal 44(5):892-898
87. Vanapalli SK, Fredlund DG, Pufahl DE (1999) The influence of soil structure and stress history on the soil–water characteristics of a compacted till. Géotechnique 49(2):143-159
88. Vardanega P, Bolton M (2013) Stiffness of Clays and Silts: Normalizing Shear Modulus and Shear Strain. Journal of Geotechnical and Geoenvironmental Engineering, ASCE 139(9):1575-1589
89. Vassallo R, Mancuso C, Vinale F (2007) Modelling the influence of stress–strain history on the initial shear stiffness of an unsaturated compacted silt. Canadian Geotechnical Journal 44(4):463-472
90. Wan RG, Guo PJ (1998) A simple constitutive model for granular soils: modified stress-dilatancy approach. Computers and Geotechnics 22(2):109-133
91. Wheeler SJ, Karube D (1996) Constitutive modelling. Proceedings of the First International Conference on Unsaturated Soil. Paris, 6-8 September.
92. Wheeler SJ, Sharma RS, Buisson MSR (2003) Coupling of hydraulic hysteresis and stress-strain behaviour in unsaturated soils. Géotechnique 53(1):41-54
93. Wheeler SJ, Sivakumar V (1995) An elasto-plastic critical state framework for unsaturated soil. Géotechnique 45(1):35-53
94. Wong KS, Mašín D (2014) Coupled hydro-mechanical model for partially saturated soils predicting small strain stiffness. Computers and Geotechnics 61:355-369

95. Wong KS, Mašín D, Ng CWW (2014) Modelling of shear stiffness of unsaturated fine grained soils at very small strains. Computers and Geotechnics 56:28-39
96. Wu SM, Gray DH, Richart Jr FE (1984) Capillary effects on dynamic modulus of sands and silts. Journal of Geotechnical Engineering 110(9):1188-1203
97. Xiong YL, Ye GL, Xie Y, Ye B, Zhang S, Zhang F (2019) A unified constitutive model for unsaturated soil under monotonic and cyclic loading. Acta Geotechnica 14(2):313-328
98. Yao Y-P, Hou W, Zhou A-N (2009) UH model: three-dimensional unified hardening model for overconsolidated clays. Geotechnique 59(5):451-469
99. Zhang J, Andrus RD, Juang CH (2005) Normalized shear modulus and material damping ratio relationships. Journal of Geotechnical and Geoenvironmental Engineering, ASCE 131(4):453-464
100. Zhou A-N, Sheng D, Sloan SW, Gens A (2012) Interpretation of unsaturated soil behaviour in the stress–saturation space: II: constitutive relationships and validations. Computers and Geotechnics 43:111-123
101. Zhou A, Sheng D (2015) An advanced hydro-mechanical constitutive model for unsaturated soils with different initial densities. Computers and Geotechnics 63:46-66
102. Zhou AN (2013) A contact angle-dependent hysteresis model for soil–water retention behaviour. Computers and Geotechnics 49:36-42
103. Zhou AN, Sheng DC, Carter JP (2012) Modelling the effect of initial density on soil-water characteristic curves. Géotechnique 62(8):669-680
104. Zhou AN, Sheng DC, Sloan SW, Gens A (2012) Interpretation of unsaturated soil behaviour in the stress–saturation space, I: volume change and water retention behaviour. Computers and Geotechnics 43:178-187
105. Zhou C (2014) Experimental study and constitutive modelling of cyclic behaviour at small strains of unsaturated silt at various temperatures. PhD thesis, Hong Kong University of Science and Technology
106. Zhou C, Ng CWW (2014) A new and simple stress-dependent water retention model for unsaturated soil. Computers and Geotechnics 62:216-222
107. Zhou C, Ng CWW (2016) Simulating the cyclic behaviour of unsaturated soil at various temperatures using a bounding surface model. Géotechnique 66(4):344-350
108. Zhou C, Ng CWW, Chen R (2015) A bounding surface plasticity model for unsaturated soil at small strains. International Journal for Numerical and Analytical Methods in Geomechanics 39(11):1141-1164

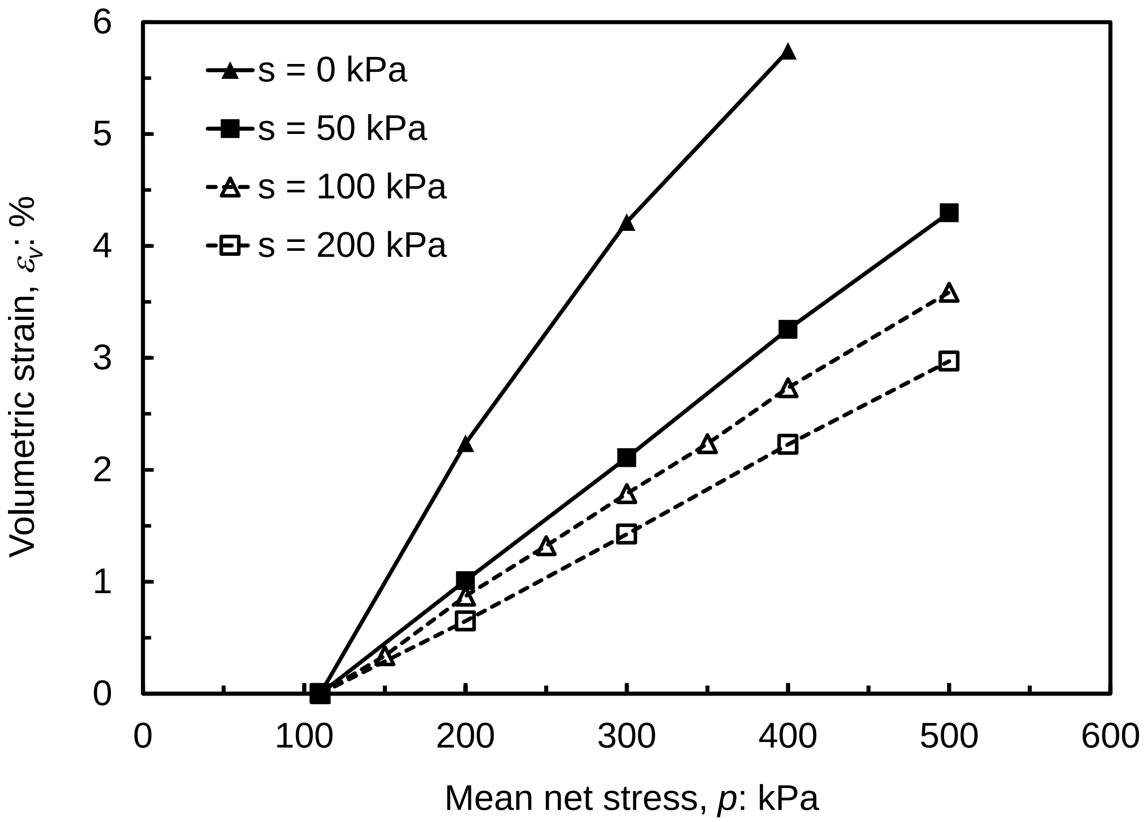

Fig. 1 Measured relationship between volumetric strain and mean net stress of a compacted silt at various suction conditions (data from Ng and Yung [64])

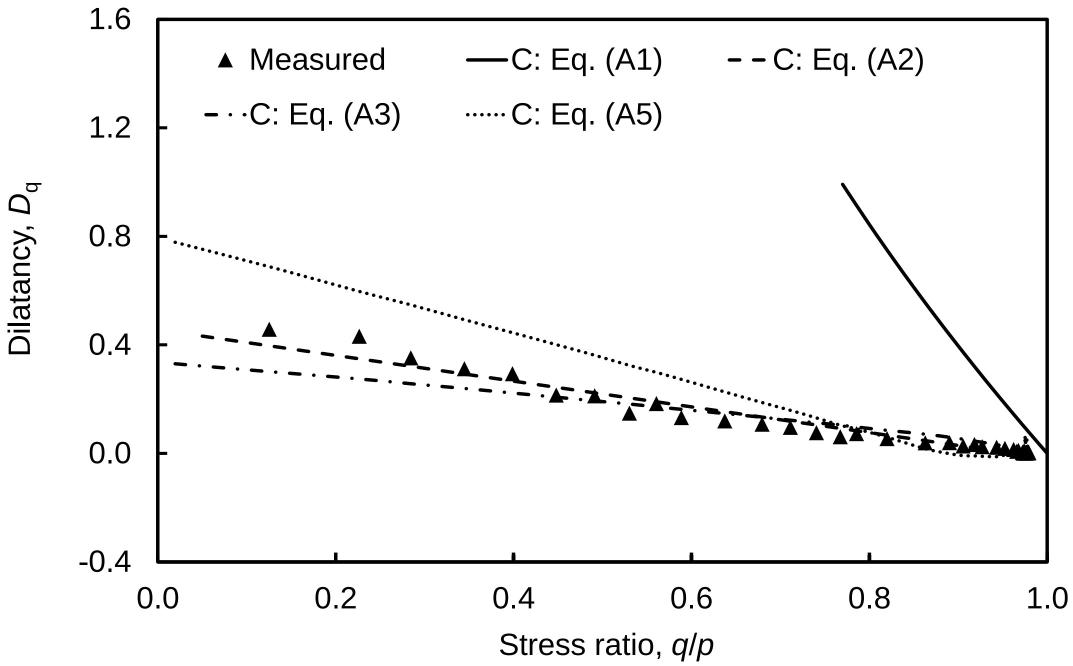

(a)

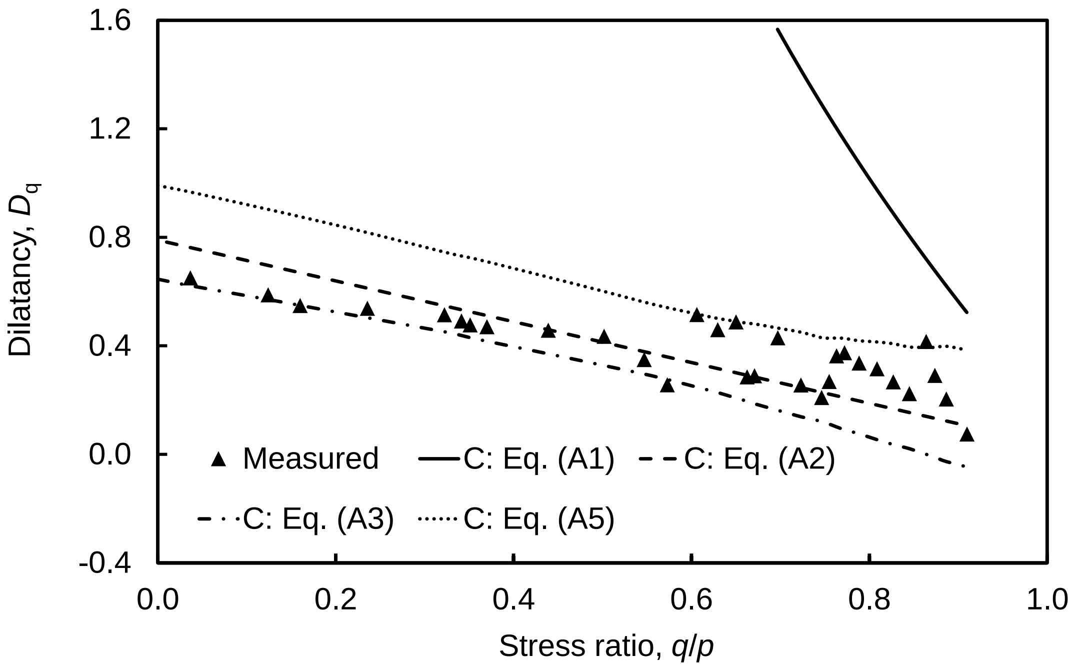

(b)

Fig. 2 Comparisons between dilatancy measured (M) [54] during shearing and theoretical results calculated (C) using the equations in Table 1: (a) s = 0; (b) s = 40 kPa

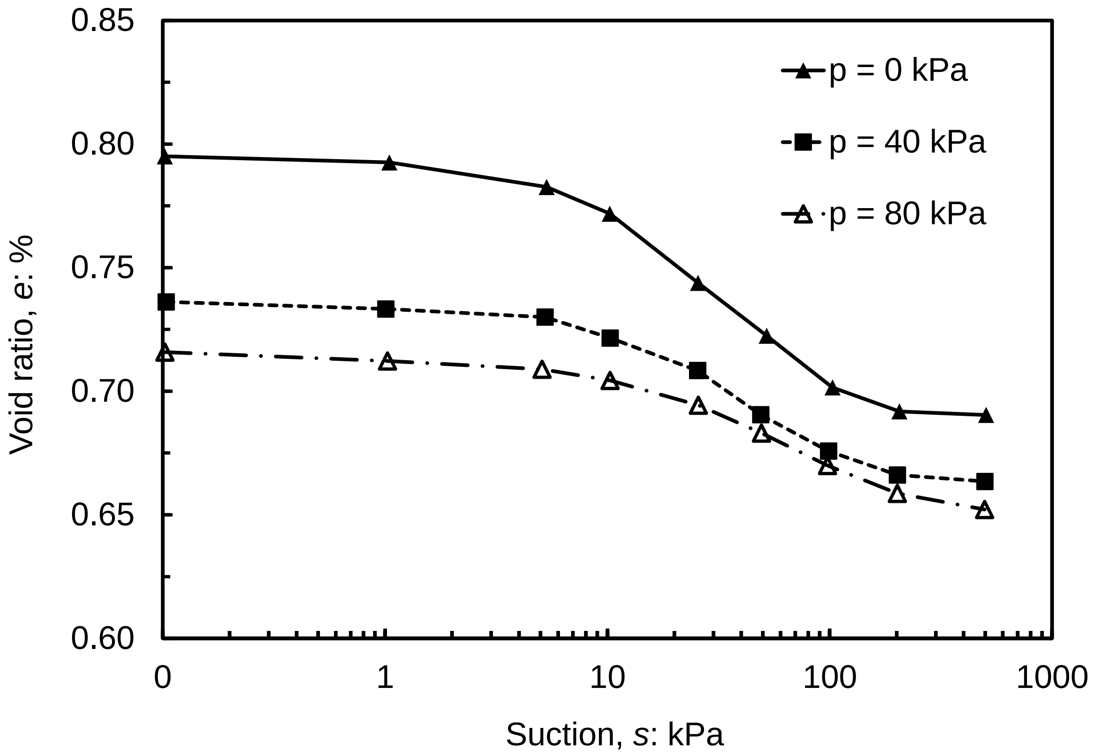

Fig. 3 Drying-induced shrinkage of a compacted silt at different mean net stresses (measured results from Chiu and Ng [14])

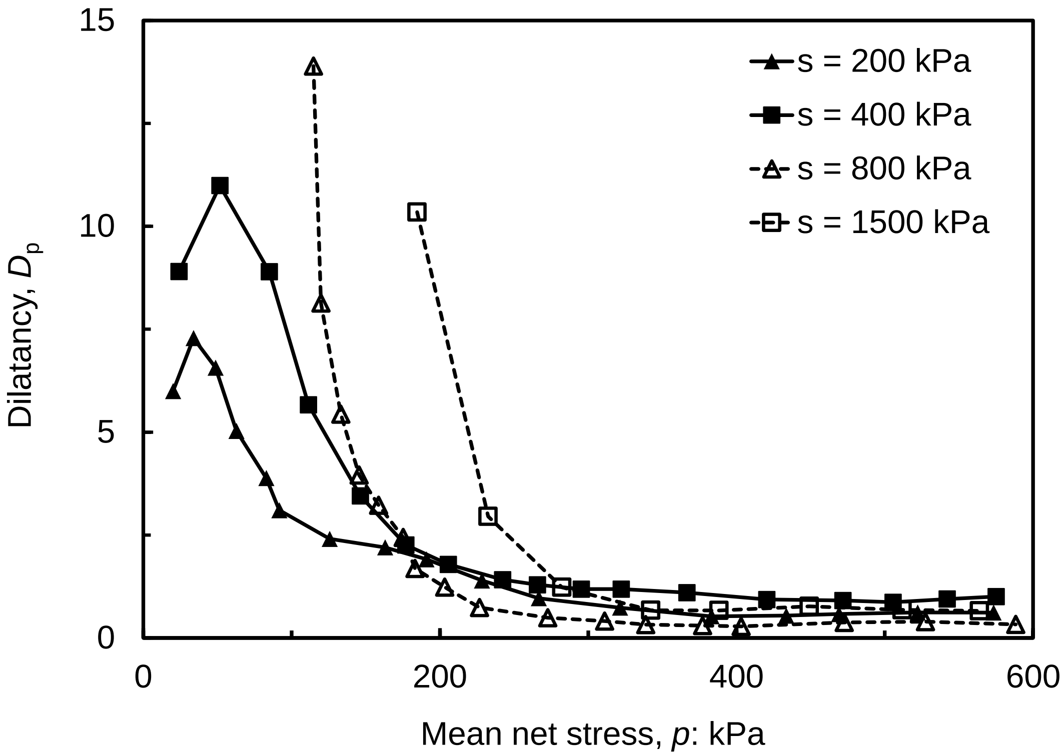

Fig. 4 Suction effects on the dilation of a compacted silt subjected to compression at a constant stress ratio (test data from Cui and Delage [18])

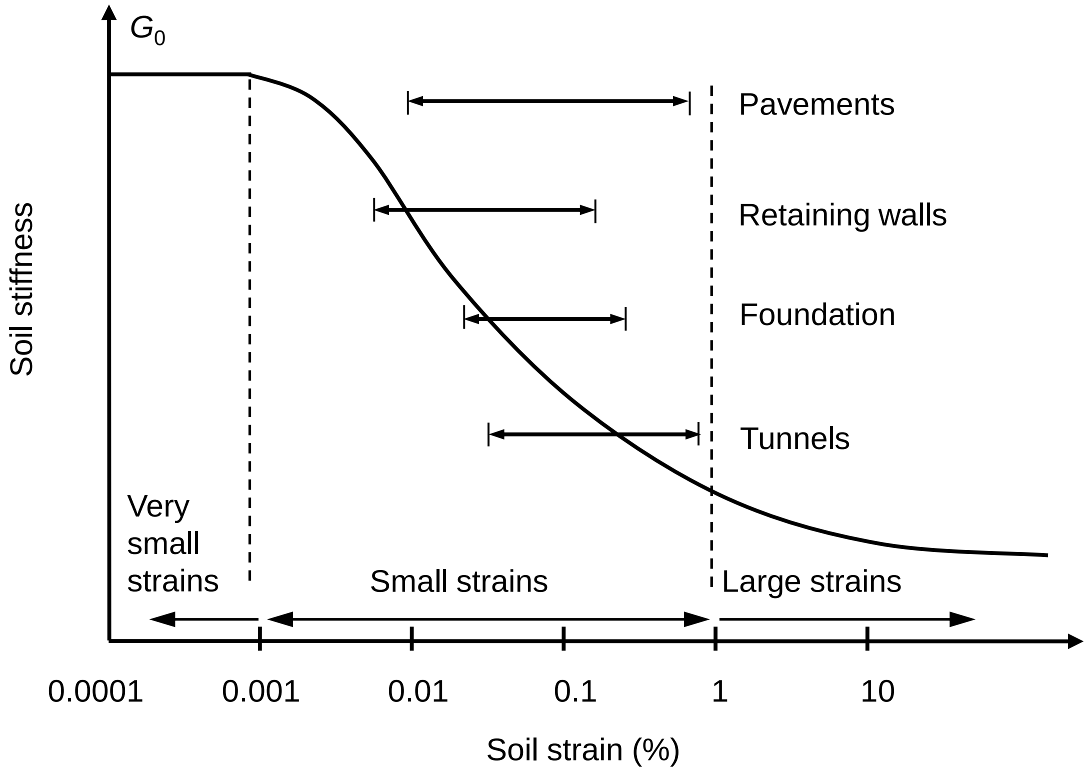

Fig. 5 Typical stiffness–strain relationship of soil (modified from Atkinson and Sallfors [4], Mair [50])

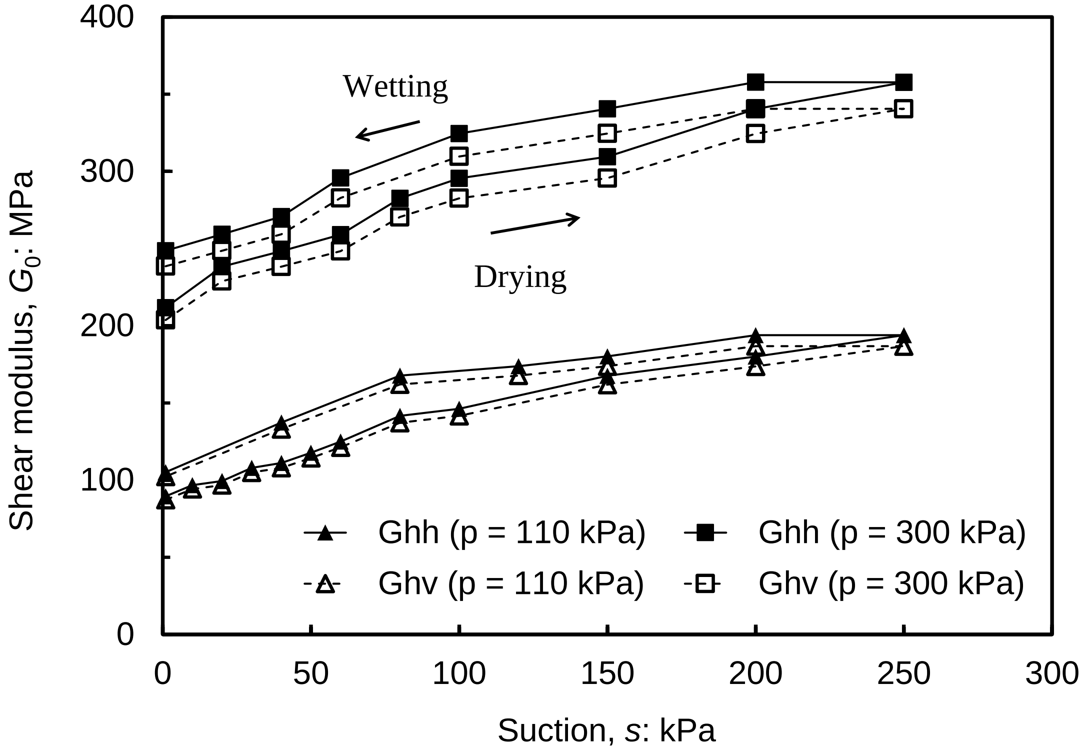

Fig. 6 Effects of suction history on anisotropic G_0 of a compacted silt (test data from Ng et al. [63])

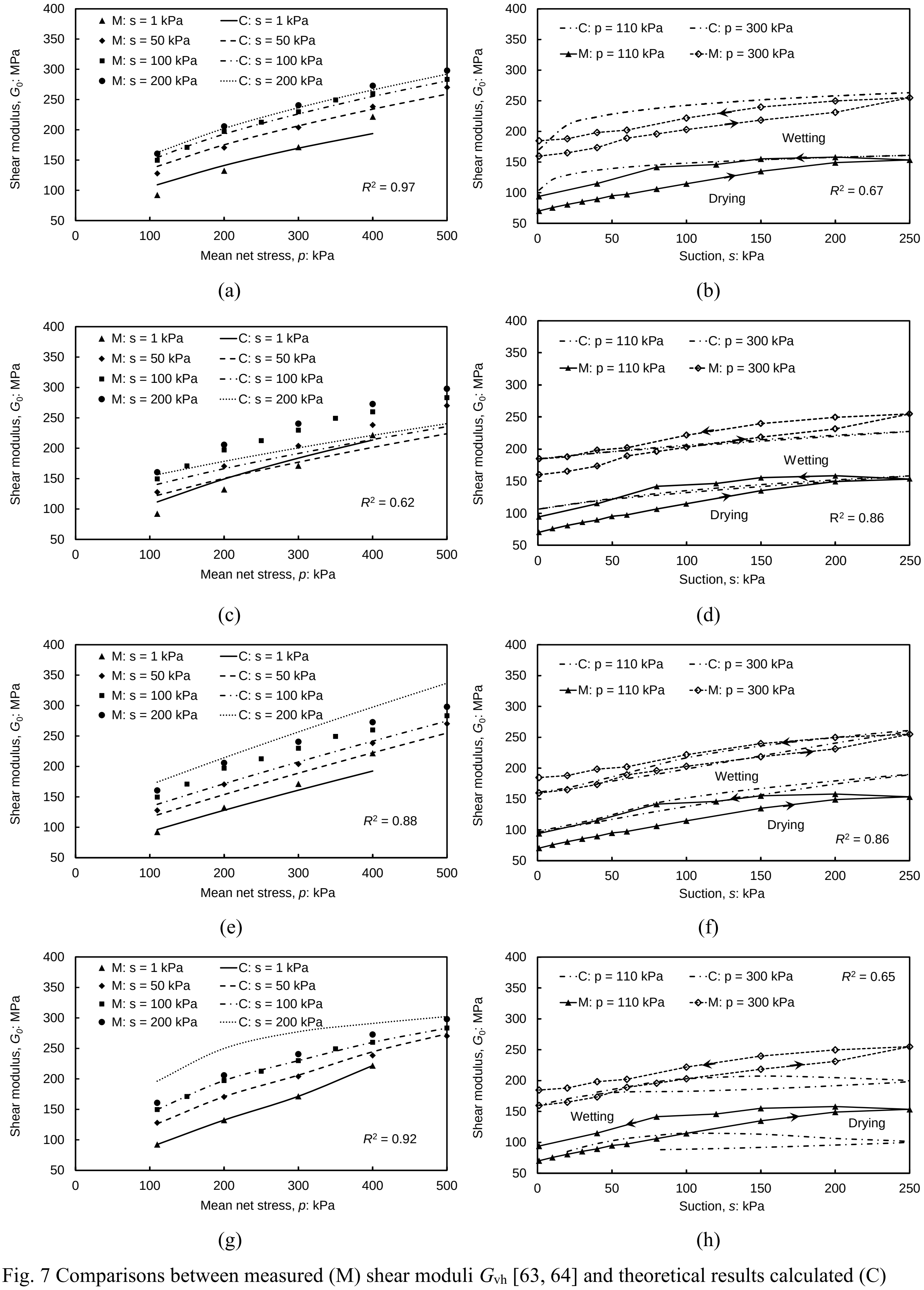

Fig. 7 Comparisons between measured (M) shear moduli G_{vh} [63, 64] and theoretical results calculated (C) using (a)-(b): equation (B2) of Ng and Yung [64]; (c)-(d): equation (B4) of Sawangsuriya et al. [78]; (e)-(f): equation (B9) of Dong et al. [20]; (g)-(h): equation (B12) of Han and Vanapalli [34]

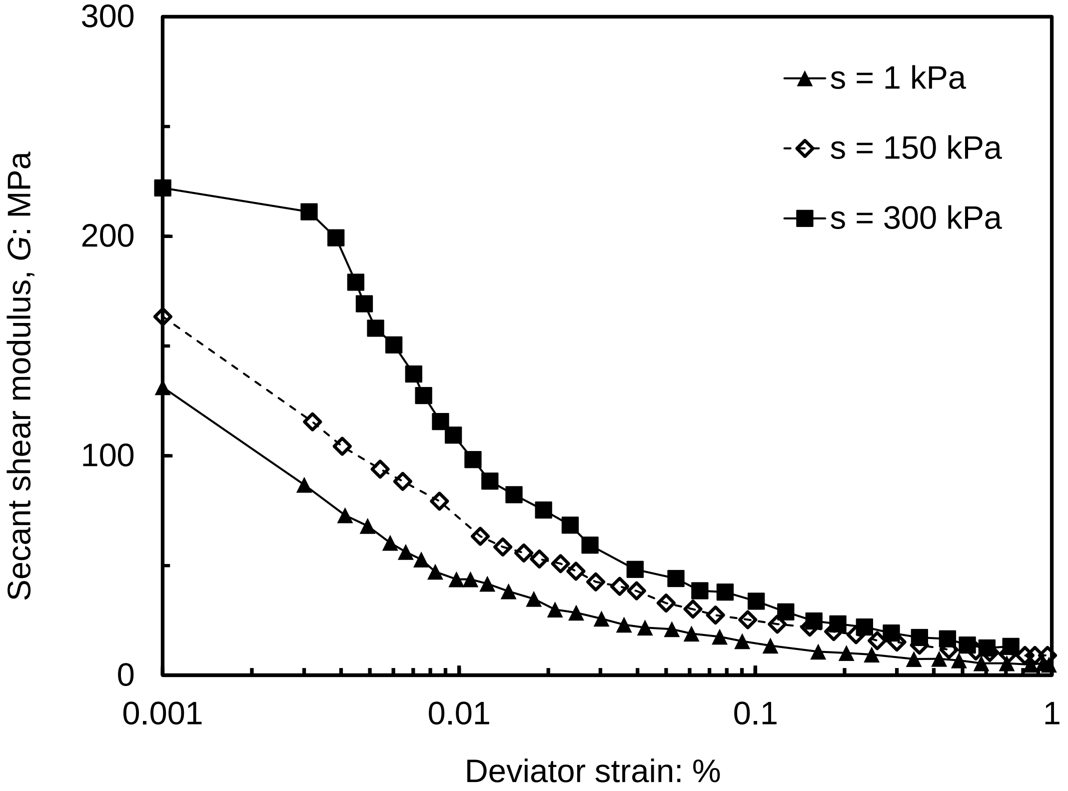

Fig. 8 Suction effects on the stiffness degradation curve of a compacted silt (test data from Ng and Xu [62])

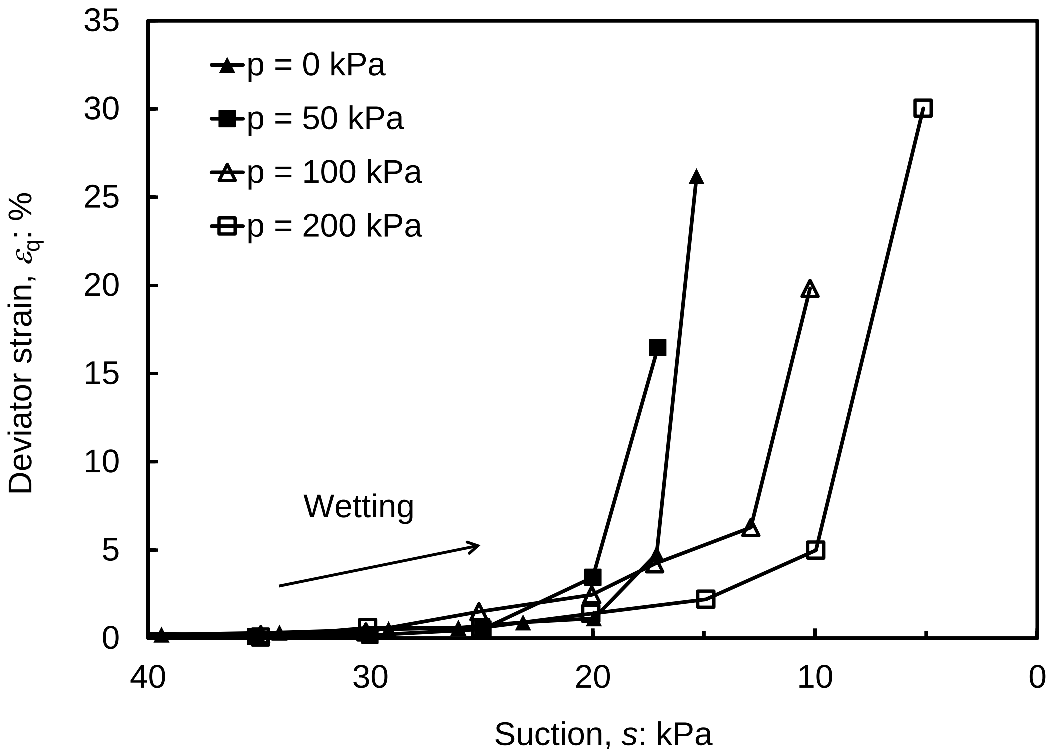

Fig. 9 Development of deviator strain of a compacted sandy silt subjected to wetting at constant *p* and *q* (test data from Ng and Chiu [54])

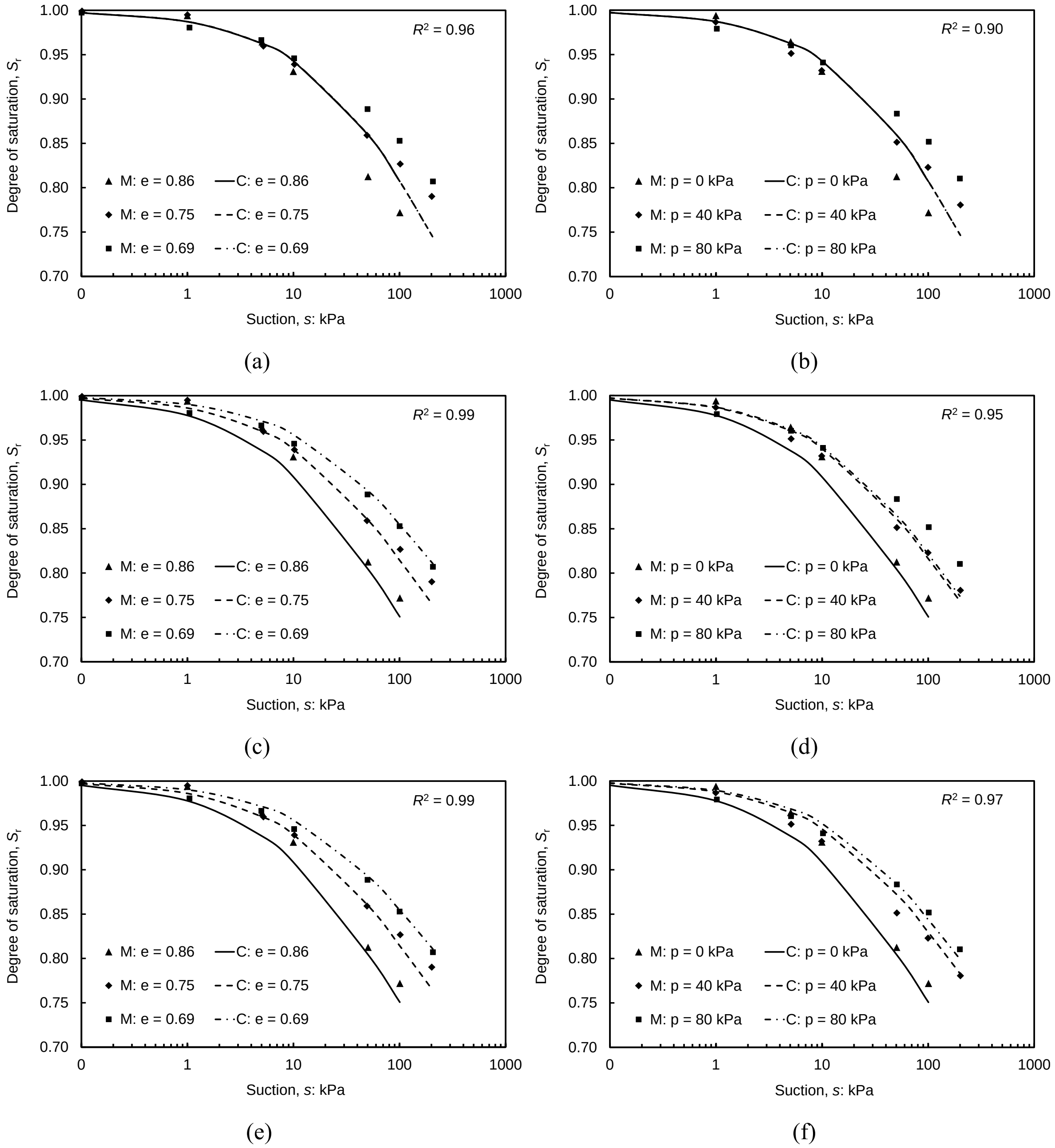

Fig. 10 Comparisons between measured (M) WRCs [59] and theoretical results calculated (C) using equations of (a)-(b): (C2) of Van Genuchten [86]; (c)-(d): (C5) of Tarantino [85]; (e)-(f): (C7) of Zhou and Ng [106]

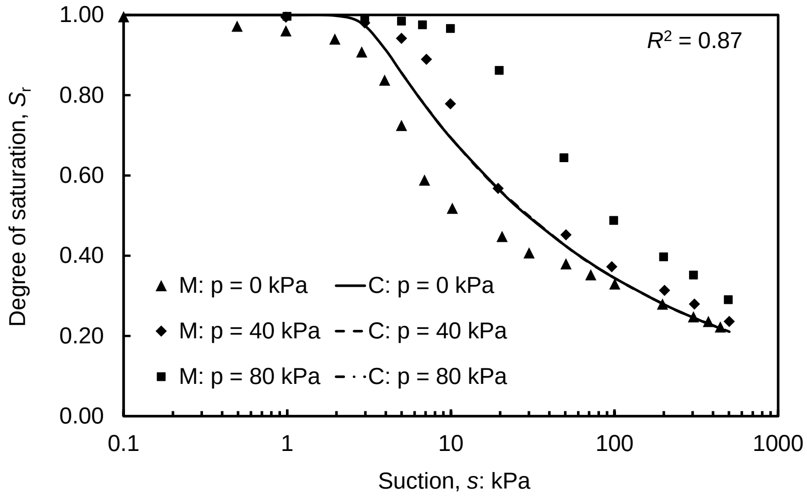

(a)

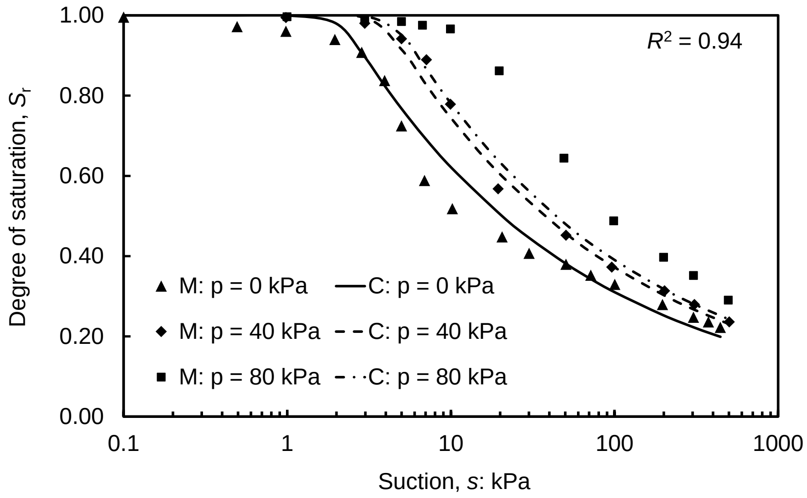

(b)

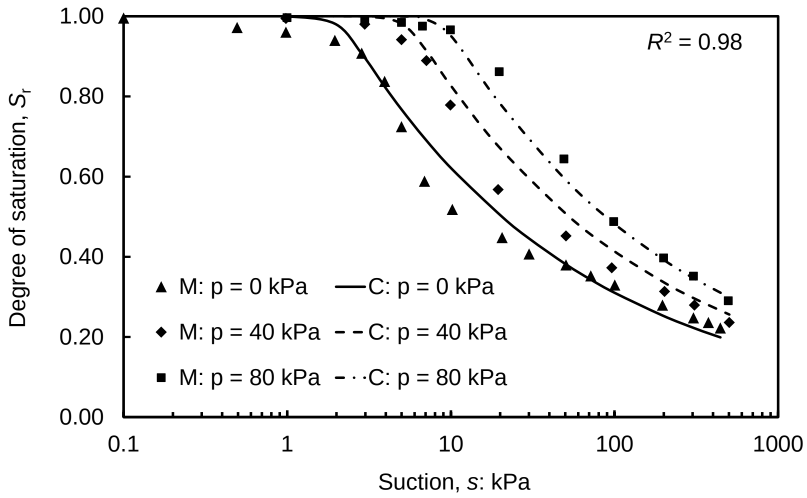

(c)

Fig. 11 Comparisons between measured (M) WRCs [42] and theoretical results calculated (C) using equations of (a): (C2) of Van Genuchten [86]; (b): (C5) of Tarantino [85]; (c): (C7) of Zhou and Ng [106]

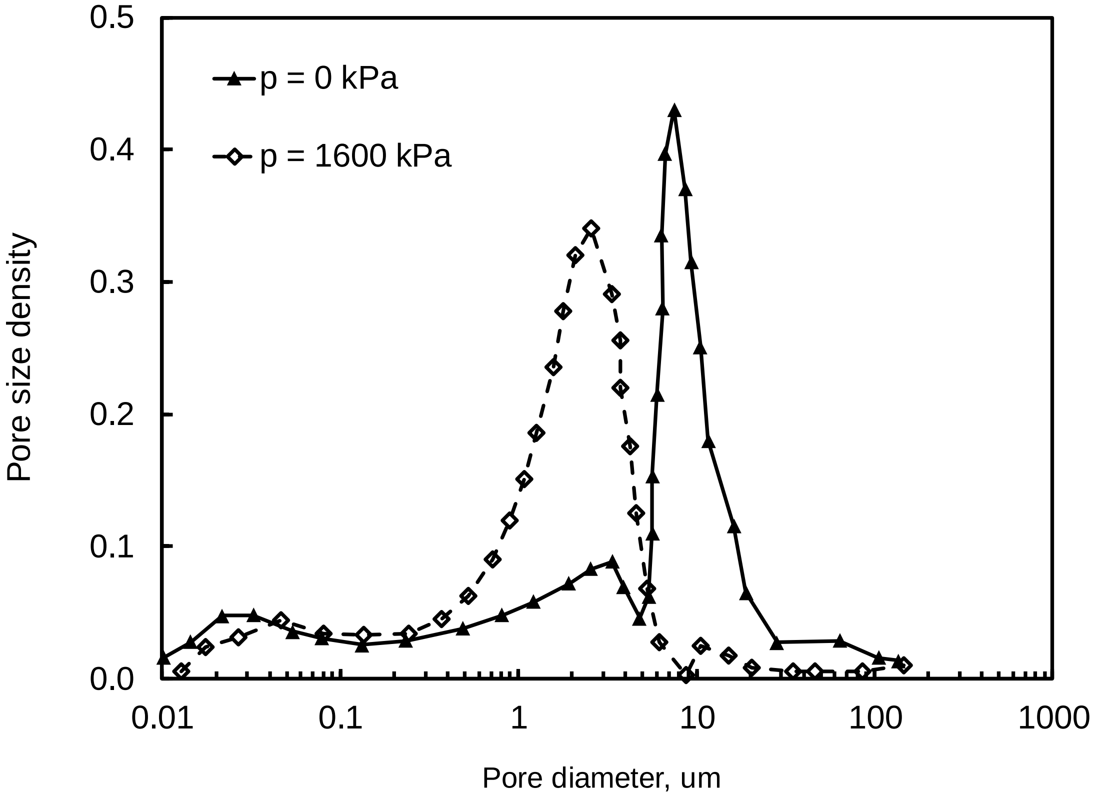

Fig. 12 Stress effects on the pore size distribution of a compacted clay with low plasticity (data from Ng et al. [60])

Table 1 Dilatancy expressions for unsaturated soils

Reference	Dilatancy expression	No.
Alonso et al. [1]	$\frac{\mathrm{d}\varepsilon_{\mathrm{p}}{}^{\mathrm{p}}}{\mathrm{d}\varepsilon_{\mathrm{q}}{}^{\mathrm{p}}} = \frac{M^2(2p + p_s - p_0)}{2\alpha q}$	A1
Cui and Delage [18]	$\frac{\mathrm{d}\varepsilon_{\mathrm{p}}{}^{\mathrm{p}}}{\mathrm{d}\varepsilon_{\mathrm{q}}{}^{\mathrm{p}}} = \frac{\eta_{\mathrm{r}} - \eta}{\mu}$	A2
Chiu and Ng [15]	$\frac{\mathrm{d}\varepsilon_{\mathrm{p}}{}^{\mathrm{p}}}{\mathrm{d}\varepsilon_{\mathrm{q}}{}^{\mathrm{p}}} = d_1(s)\left(e^{m\psi} - \frac{\eta}{M}\right)$	A3
Russell and Khalili [77]	$\frac{\mathrm{d}\varepsilon_{\mathrm{p}}{}^{\mathrm{p}}}{\mathrm{d}\varepsilon_{\mathrm{q}}{}^{\mathrm{p}}} = (1 + k_{\mathrm{d}} \cdot \psi)\mathrm{M} - \eta$	A4
Chávez and Alonso [9]	$\sin\varphi_{\mathrm{m}} = \frac{sin\phi_{\mathrm{m}} - \left(\frac{e}{e_{\mathrm{cr}}}\right)^{\beta} sin\phi_{\mathrm{cr}}}{1 - \left(\frac{e}{e_{\mathrm{cr}}}\right)^{\beta} sin\phi_{\mathrm{m}} sin\phi_{\mathrm{cr}}}$	A5
Alonso et al. [2]	$\frac{\mathrm{d}\varepsilon_{\mathrm{p}}{}^{\mathrm{p}}}{\mathrm{d}\varepsilon_{\mathrm{q}}{}^{\mathrm{p}}} = \left(a + \frac{b}{\left(\eta W^P / p\right)^2}\right)^2 - b^2$	A6

Table 2 Model parameters for numerical simulations in Fig. 2

Equation	s = 0 kPa	s = 40 kPa
A1	M = 1.55	M = 1.55, p_s = 4.5 kPa
A2	η_r = 1.55, μ = 3.36	η_r = 1.62, μ = 2.05
A3	M = 1.55, d_1 = 0.2, m = 5 Γ = 0.824, λ = 0.11	M = 1.55, c = 7 kPa , d_1 = 0.6, m = 5 Γ = 0.982, λ = 0.186
A4	sin ϕ_{cr} = 0.616, β = -2.5 Γ = 0.824, λ = 0.11	sin ϕ_{cr} = 0.638, β = -2.5 Γ = 0.982, λ = 0.186

Note: critical state line is modelled using $q = Mp + c$ and $e = \Gamma - \lambda \cdot \ln\left(\frac{p}{p_{at}}\right)$ where p_{at} = 100 kPa.

Table 3 Stiffness expressions for unsaturated soils

Model type	Reference	Stiffness expression	No.
I	Leong et al. [43]	$G_0 = (G_0)_{\mathrm{ref}}(1 + [(\sigma_3 - u_\mathrm{a})/p_{\mathrm{atm}}]^n)\left(1 + ln(1 + s/p_{\mathrm{atm}})\right)^m$	B1
	Ng and Yung [64]	$G_{0(\mathrm{ij})} = C_{\mathrm{ij}}^2 f(e)\left[(\sigma_\mathrm{i} - u_\mathrm{a})/p_{\mathrm{atm}} \cdot (\sigma_\mathrm{j} - u_\mathrm{a})/p_\mathrm{r}\right]^n (1 + s/p_\mathrm{r})^{2m}$ where $p_\mathrm{r} = 1\ kPa$	B2
	Sawangsuriya et al. [78]	$G_0 = Af(e)(\sigma - u_\mathrm{a})^n + C(S_\mathrm{r})^\kappa s$	B3
II	Sawangsuriya et al. [78]	$G_0 = Af(e)[(\sigma - u_\mathrm{a}) + (S_\mathrm{r})^\kappa s]^n$	B4
	Pagano et al. [72]	$G_0 = \frac{2}{7}\frac{l^2}{V}\frac{3}{2}k_{n_0}^{2/3}\left[\frac{\sigma_\mathrm{i}}{2l}V\right]^{1/3}$ where $\sigma_\mathrm{i} = \sigma + \sigma_\mathrm{i}^\mathrm{b}\left(\frac{S_\mathrm{r} - S_\mathrm{rm}}{1 - S_\mathrm{rm}}\right) + \sigma_\mathrm{i}^\mathrm{b}\left(1 - \frac{S_\mathrm{r} - S_\mathrm{rm}}{1 - S_\mathrm{rm}}\right)$	B5
III	Sawangsuriya et al. [78]	$G_0 = Ap_{\mathrm{atm}}\left[\frac{{p_c}'_0}{p_0}exp\left(\frac{\Delta e^p}{\lambda - \kappa}\right)\right]^K \left[\frac{p_n}{p'}exp\left(b(S_{\mathrm{e0}} - S_\mathrm{e})\right)\right]^K \left(\frac{p'}{p_{\mathrm{atm}}}\right)^n$ where $p' = p_\mathrm{n} + \frac{S_\mathrm{r} - S_{\mathrm{r,res}}}{1 - S_{\mathrm{r,res}}}s$	B6
	Biglari et al. [7]	$G_0 = A(p_{\mathrm{atm}})^{1-n} f(e) OCR^m (p + sS_\mathrm{r})^n\left[1 - a\left(1 - exp(b\xi)\right)\right]$	B7
	Wong et al. [95]	$G_0 = Ap_\mathrm{r} f(e)(p'/p_\mathrm{r})^n S_\mathrm{r}^{-k/\lambda}$ where $p' = p + (s_\mathrm{e}/s)^{0.55}s$	B8
	Dong et al. [20]	$G_0 = G_0\ (1/s_\mathrm{e})^a(1 + \sigma'/p_{\mathrm{atm}})^b$ where $\sigma' = (\sigma - u_\mathrm{a}) + S_\mathrm{e}s$	B9
IV	Wu et al. [96]	$G_0 = G_0^{\mathrm{dry}}\left(1 + H(S_\mathrm{r})\right)$	B10
	Mancuso et al. [51]	$G_0 = G_{0(s*)}\left[(1 - r)exp\left(-\beta(s - s*)\right) + r\right]$	B11
	Han and Vanapalli [34]	$G_0 = G_0^{\mathrm{sat}} + \left(G_0^{\mathrm{ref}} - G_0^{\mathrm{sat}}\right)(s/s_{\mathrm{ref}})\left(S_\mathrm{r}/S_{\mathrm{r,ref}}\right)^\xi$	B12

Table 4 Model parameters for numerical simulations in Fig. 7

Equation	Value of model parameters
B2	$C_{\mathrm{vh}} = 11\ MPa;\ n = 0.17, m = 0.045$
B4	$A = 9\ MPa;\ n = 0.4, \kappa = 0.3$
B9	$G_0 = 53\ MPa;\ n = 0.4, m = 0.8$
B13	$\xi = 2;\ s_{\mathrm{ref}} = 100\ kPa$ Other variables G_0^{sat}, G_0^{ref}, S_{r}, $S_{\mathrm{r,ref}}$ depends on suctions and stresses. The measured results for them are used in the numerical simulation.

Note: the same void ratio function $1/(0.3 + 0.7e^2)$ is used in all equations, considering that the current study focuses on stress and suction effects on G_0.

Table 5 SWRC expressions for unsaturated soils

Model type	Reference	SWRC expression	No.
I	Gardner [30]	$S_r = \frac{1}{1 + as^n}$	C1
	Van Genuchten [86]	$S_r = \left(1 + \left(\frac{s}{a}\right)^{m_2}\right)^{-m_1}$	C2
	Fredlund and Xing [23]	$S_r = \left(ln\left(2.7 + \left(\frac{s}{a}\right)^n\right)\right)^{-m}$	C3
II	Gallipoli et al. [27]	$S_r = \left(1 + \left(\frac{se^{m_4}}{m_3}\right)^{m_2}\right)^{-m_1}$	C4
	Tarantino [85]	$S_r = \left(1 + \left(\frac{se^{m_4}}{m_3}\right)^{m_2}\right)^{-m_1}$ where $m_4 = 1/m_1/m_2$	C5
	Sheng and Zhou [83]	$\mathrm{d}S_{\mathrm{r}} = \mathrm{E} - \mathrm{B}\frac{S_{\mathrm{r}}}{n}(1 - S_{\mathrm{r}})^{\xi}\mathrm{d}s - \frac{S_{\mathrm{r}}}{e}(1 - S_{\mathrm{r}})^{\xi}\mathrm{d}e$	C6
III	Zhou and Ng [106]	$S_{\mathrm{r}} = \left(1 + \left(\frac{s\left(e_0 - \alpha_{\mathrm{p}}\ln(1 + p/p_{\mathrm{atm}}) - \alpha_{\mathrm{s}}\ln(1 + s/p_{\mathrm{atm}})\right)^{m_4}}{m_3(1 + p/p_{\mathrm{atm}})^{m_5}}\right)^{m_2}\right)^{-m_1}$ where $m_4 = 1/m_1/m_2$	C7

Table 6 Model parameters for numerical simulations in Fig. 10 and Fig. 11

Equation	Test by Ng and Pang [59]	Test by Lee et al. [42]
C2*	$m_1 = 0.26, m_2 = 0.7, m_3 = 13\ kPa$, $m_5 = 0.5$	$m_1 = 0.04, m_2 = 7.6, m_3 = 0.31\ kPa$, $m_5 = 0.5$
C5	$m_1 = 0.26, m_2 = 0.7, m_3 = 13\ kPa$	$m_1 = 0.04, m_2 = 7.6, m_3 = 0.31\ kPa$
C7	$m_1 = 0.26, m_2 = 0.7, m_3 = 70\ kPa$	$m_1 = 0.04, m_2 = 7.6, m_3 = 3\ kPa$

Note: * Measured void